Chapter 7
Analysis of Brain Recurrence

Clifton Frilot II, Paul Y. Kim, Simona Carrubba, David E. McCarty, Andrew L. Chesson Jr., and Andrew A. Marino

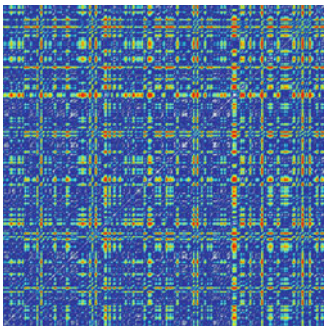

Abstract Analysis of Brain Recurrence (ABR) is a method for extracting physiologically significant information from the electroencephalogram (EEG), a non-stationary electrical output of the brain, the ultimate complex dynamical system. ABR permits quantification of temporal patterns in the EEG produced by the non-autonomous differential laws that govern brain metabolism. In the context of appropriate experimental and statistical designs, ABR is ideally suited to the task of interpreting the EEG. Present applications of ABR include discovery of a human magnetic sense, increased mechanistic understanding of neuronal membrane processes, diagnosis of degenerative neurological disease, detection of changes in brain metabolism caused by weak environmental electromagnetic fields, objective characterization of the quality of human sleep, and evaluation of sleep disorders. ABR has important beneficial implications for the development of clinical and experimental neuroscience.

C. Frilot II
School of Allied Health Professions, LSU Health Sciences Center, Shreveport, LA, USA

P.Y. Kim • D.E. McCarty • A.L. Chesson Jr. • A.A. Marino (✉)
Department of Neurology, LSU Health Sciences Center, P.O. Box 33932, Shreveport, LA 71130-3932, USA
e-mail: andrewamarino@gmail.com

S. Carrubba
Natural Sciences Department, Daemen College, Amherst, NY, USA

C.L. Webber, Jr. and N. Marwan (eds.), *Recurrence Quantification Analysis*, Understanding Complex Systems, DOI 10.1007/978-3-319-07155-8_7,

Abbreviations

ABR	Analysis of brain recurrence
AHI	Apnea–hypopnea index
ARA	Aperiodic rhythmic activity
EEG	Electroencephalogram
EEP	Electrosensory evoked potential
EMF	Electromagnetic field
EP	Evoked potential
FZAC	First zero of the autocorrelation function
MEP	Magnetosensory evoked potential
MS	Multiple sclerosis
REM	Rapid eye movement
WASO	Wake after sleep onset

7.1 Introduction

Human behaviors including somatic, cognitive, and emotional responses to stimuli, therapeutic reactions to drugs, and changes in signs or symptoms during progression of acute and chronic diseases are all mediated and controlled by the brain. Even though its structural complexity is daunting and its differential laws are mysterious, we accept the idea that the brain always acts lawfully. How it does so has been a perennial subject of scientific and philosophical interest.

In principle, the task of explaining the behaviors could be approached by attempting to deduce equations of motion, akin to the Hamiltonian formulation of mechanics, or by following a statistical approach similar to the determination of the pressure in a vessel by averaging over many atomic-level motions. But brain activity is such a complicated process that we have nil expectation it can be profitably analyzed by means of these traditional approaches. But even though we cannot deduce the brain's governing differential laws, we are certain that they exist, because the behaviors governed by brain activity are lawful, not random.

Even though the task of understanding brain function as a necessary consequence of its differential laws is probably impossible, other goals regarding brain function can be achieved. An ability to make reliable predictions of human behaviors has enormous practical benefits in the fields of translational medicine and experimental neuroscience, even if the predictions are only probabilistic. Our primary goal here is to show how recurrence analysis, when employed in the context of an appropriate experimental and statistical framework, a technique we call *Analysis of Brain Recurrence* (ABR), yields such benefits.

In the next section we provide foundational information regarding the structure and function of the brain, with emphasis on the *complexity conjecture*, a fundamental principle that undergirds the unique applicability of recurrence analysis to

the study of brain activity. We shall see why recurrence analysis is extraordinarily well-suited for brain studies.

The following section describes the origin of recurrence analysis and what it is when looked at from the perspective of brain studies. Recurrence analysis is a remarkable invention that stemmed from the keen insight that biological systems are not crude versions of physical systems but rather irreducibly complex systems whose understanding for useful purposes requires novel analytical methods. The basic properties of recurrence analysis are discussed, and its ability to detect law-governed activity is demonstrated.

Next we present the results of published studies that encompass our applications of ABR. They include discovery of a human magnetic sense, the diagnosis of multiple sclerosis, detection of changes in brain metabolism caused by weak electromagnetic fields (EMFs), insights into the biophysical and physiological bases of EMF transduction, and applications to the objective characterization of sleep and the diagnosis of sleep disorders. Recurrence analysis must be employed in an appropriate statistical context to permit its results to go beyond geometric curiosities and reliably generalize to real-world problems. Consequently the true error rates for the hypotheses tested are listed, and references are provided to the original descriptions for the statistical details. The applications of ABR chosen for discussion should give the reader a good idea of its capabilities and limitations.

In the final section we attempt to place ABR in the general context of the scientific method so that the rock-solid foundation of ABR is clear. In contrast with attempts to explain the world in terms of time-reversible linear differential laws, ABR has different goals, makes opposite assumptions, and yields rewards not otherwise obtainable.

7.2 The Brain

7.2.1 Physiological Role

The brain is an open system that constantly interacts with the environment and incessantly changes, always existing in far-from-equilibrium states (Fig. 7.1). A continuous flow of mass, energy, and information crosses the skin and drives the brain's ceaseless activity, which occurs during the presence and absence of recognizable stimuli and ceases only in death. The brain generates information and also changes its internally-generated programs in response to information obtained from the environment. These processes embed the world in a unique context for each individual, determined by time and experience. The brain's governing laws are necessarily nonlinear and non-autonomous, because linear and/or autonomous systems don't move or change themselves or exhibit irreversible changes.

The physical appearance of the brain belies its abilities. The brain is small, about 0.34 kg at birth, 1.4 kg at maturity, 1.3 kg in advanced old age [1], and easily

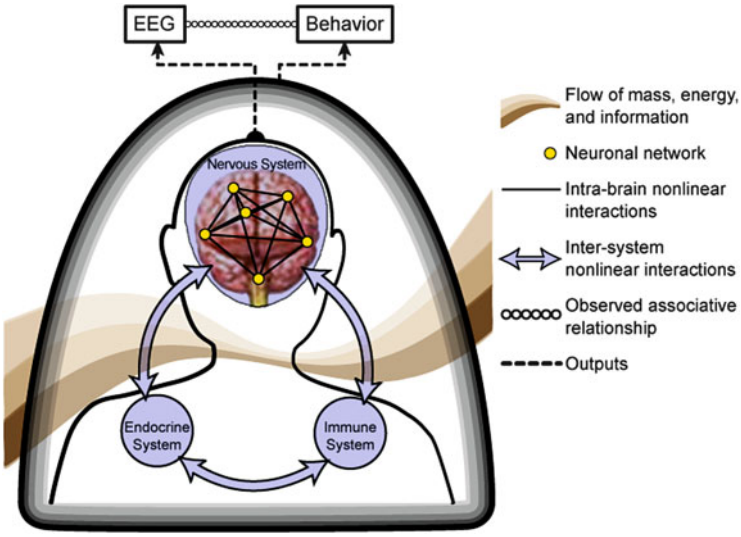

Fig. 7.1 Continuous flows of mass, energy, and information drive the brain's master-control function, which is the governance of the body's three main regulatory systems. Facilitated by interactions among a relatively small number of local neuronal networks, the brain receives numerous chemical and energetic inputs, and produces numerous outputs. The interactions determine all observable responses and behaviors, including the electroencephalogram (EEG). We regard observations and their contemporaneous EEGs as physiological doppelgangers that code for each other

deformed, like a gel. The brain's abilities ultimately arise from the conjoint operation of the laws of mechanics, electricity, and thermodynamics in the context of what is probably the most complex structure in the universe. The brain's cellularity and microscopic anatomy consists of $\sim 10^{11}$ distinct cells called neurons, with $\sim 10^{14}$ contacts between them [2], all of which are self-organized into $\sim 10^{2}$ structural and functional networks that are fed and nurtured by $\sim 10^{12}$ support cells of various types [3]. Information transfer at the neuronal level is reasonably well understood conceptually in terms of neurotransmitters, neuromodulators, cytokines, direct electrical communication between cell interiors via gap junctions, and electrotonic conduction through the extracellular fluid [4]. Some phenomenological descriptions of neuronal signaling have been developed, the Hodgkin–Huxley equations for example, but there are no direct explanations based on general laws.

At the organ level almost nothing is known about what governs brain activity, and we lack even phenomenological descriptions. Explaining human behaviors at the level of individuals is therefore problematical. Nevertheless each brain signs itself by producing an electroencephalogram (EEG), a time-dependent voltage signal conventionally measured on the scalp (Fig. 7.2) (measurable anywhere on the skin but with reduced sensitivity because of the passive electrical properties of tissue).

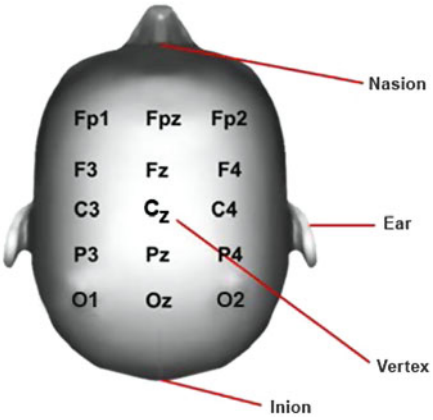

Fig. 7.2 Scalp locations and labels for EEG measurements (10–20 system). The EEG is measured at standardized locations on or symmetrically distributed about the mid-sagittal plane [5]. The locations are identified by rules based on proportional distance measurements made in relation to arcs between the nasion and inion, and between the ears

7.2.2 The Baseline EEG

The EEG (Fig. 7.2) is an emergent property of the dynamical activity of the brain, and consequently has no specific origin, like a smile. We conceptualize the EEG as a state property of the brain in the sense that some of the information it contains involves the cooperative activity of all its cells. In principle, an EEG measured during an arbitrary time interval would have been different if even one neuron had died immediately prior to the beginning of the interval.

The spectral energy in the EEG occurs almost entirely below 50 Hz. The signal therefore cannot directly reflect rapid electrophysiological events occurring at the neuronal membrane [4]. Attempts to interpret the EEG in relation to phenomena associated with higher organizational levels have traditionally been based on use of the root mean square of the signal (time averaging), or on its Fourier decomposition with subsequent determinations of relative power in standard frequency intervals (spectral analysis). The variables associated with both methods were assumed to be classical stochastic variables (described by fixed probability distributions). Unfortunately the EEG is dramatically non-stationary over the time scales pertinent to the problem of interpreting the EEG (Fig. 7.3). This salient fact conflicts with the logic of linear methods like time averaging and spectral analysis. Valid use of these methods requires that differences in means of dependent variables arise solely from changes in the independent variables, not from changes in the dynamical law of the system. But that is exactly what occurs in the brain, evidenced by the nonstationarity of the EEG (Fig. 7.3). In marked contrast, stochasticity is irrelevant to the validity of ABR. Indeed, its fundamental value is that it permits characterization of the brain's non-autonomous activity, which is where human behaviors actually come from (see below).

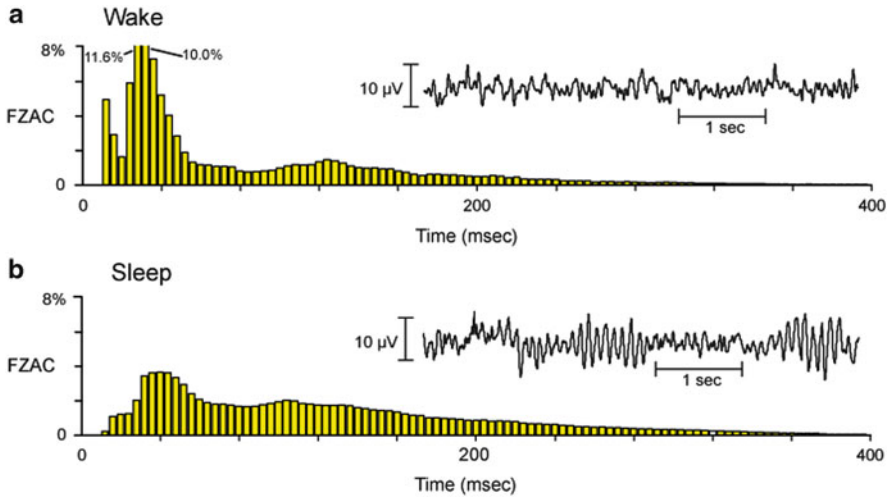

Fig. 7.3 Nonstationarity in the human EEG during wake and sleep. (**a**) EEGs were recorded for 5 min (O1, O2, P3, P4, C3, C4) from each of ten vigilant subjects, and the first zero of the autocorrelation function (FZAC) was determined second-by-second. The results (∼1,800 values/subject) were divided into 4-ms bins, averaged, and the resulting histogram was normalized. (**b**) EEGs (from C3) were recorded for 7–8 h from each of ten sleeping subjects, and the mean normalized FZAC histogram (∼28,000 values/subject) was determined. The histograms of the EEG during both wake and sleep indicate that the statistical properties of the EEG change drastically from second to second, which is the definition of a nonstationary time series. The nonstationary character of the EEG implies that brain activity is governed by non-autonomous differential laws. Sampling rate, 500 Hz

7.2.3 The Stimulated EEG

Somatic and/or cognitive stimuli produce transient stereotyped electrophysiological responses in the EEG called evoked potential (EPs), typically lasting 100–400 ms and occurring 100–400 ms after application of the stimulus [6,7]. Stimuli trigger both onset and offset responses, respectively caused by the onset and offset of the stimulus. For example a light pulse from a light-emitting diode has an onset and offset whose durations are the rise- and fall-times of the diode current, respectively, and both aspects of the stimulus trigger an EP. Different sets of neuronal networks are involved in attention to stimuli onset and offset [8–11]. The EPs are much weaker than the baseline EEG, with which they become convolved.

Evoked potentials have traditionally been detected by time averaging the EEG over intervals immediately following N application of the stimulus. The procedure results in an increase in signal (the EP) to noise (the EEG) $\propto \sqrt{N}$. Evoked potentials not time-locked to the stimulus are undetectable by time averaging, and hence were essentially unknown prior to the development of recurrence analysis (see below).

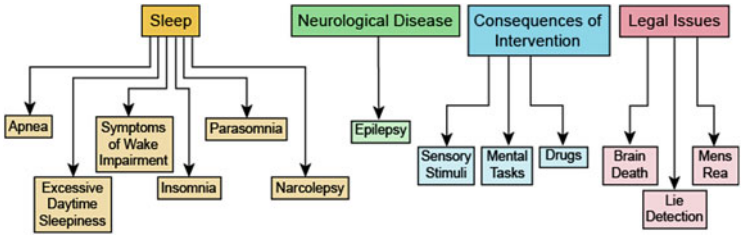

Fig. 7.4 Present uses of the EEG

7.2.4 Uses of EEG

The main clinical use of EEGs occurs in sleep medicine, where measurements are typically made from six derivations during overnight studies for use in characterizing the stages of sleep (typically, the first step in diagnosing sleep disorders) (Fig. 7.4). With the exception of epilepsy, EEG measurements play a minor role in diagnosis of neurological diseases, having largely been supplanted by magnetic resonance imaging. Evoked potentials are used clinically to evaluate the occurrence of lesions in the peripheral nervous system. Robust utilization of EPs occurs in experimental neuroscience because EPs are the only known method for objectively characterizing the functional activity of the brain over times on the order of milliseconds. In principle, the guilty mind (*mens rea*) and the lying witness can be detected based on EEG analysis, but efforts to do so have been unsuccessful. The absence of an EEG for a defined interval is a common basis for recognizing death.

Following the development of the theory of low-dimensional nonlinear dynamics, interest spiked in the possibility that the theory was directly applicable to the EEG. Reports describing calculations of fractal dimension and Lyapunov exponents were interpreted as evidence that the brain was a low-dimensional nonlinear system operating in the chaotic mode, like the Lorenz model of weather [12]. But the effort to show that EEGs were outputs of low-dimensional systems of the type for which the theory was created ultimately failed [13]. Nevertheless new initiatives developed, prompted by a dawning recognition that progress regarding understanding the lawfulness of the brain required approaches that were beyond linear and low-dimensional nonlinear approximations, and more faithfully mirrored the brain's actual nonlinear dynamics, namely that it is governed by non-autonomous differential laws, and probably has dimensions closer to 10^{10} than to 10. As we shall see, ABR uniquely accomplished the task of revealing the footprints of the laws.

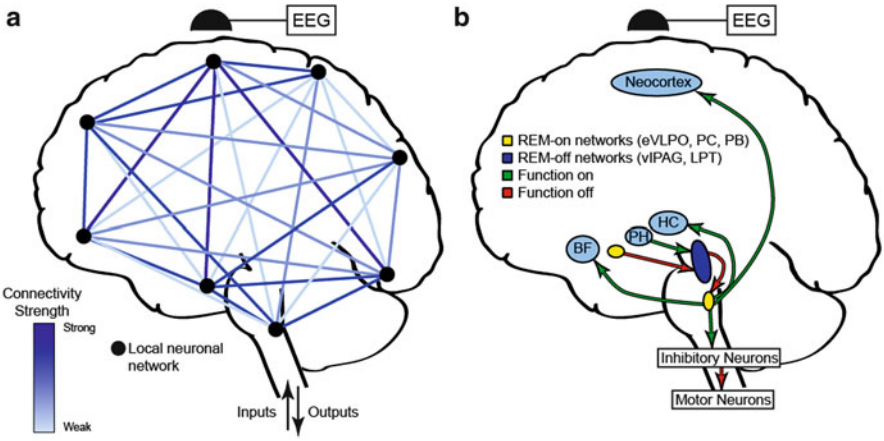

Fig. 7.5 The complexity conjecture regarding the origin of the human EEG. (**a**) Brain function is mediated by electrical activity in localized neuronal networks and their dynamic internetwork electrical connectivity, which result from synaptic and non-synaptic processes [4]. The instantaneous strength of the connectivity between local networks is represented by the color intensity of the line that joins them. The EEG measured for any Δt from any derivation characterizes the entire brain (brain state) during Δt. In practice, the time interval regarded as the characteristic duration of the state is chosen in relation to the behavior of interest. As examples, $\Delta t \approx 100$ ms for detecting evoked potentials, and $\Delta t = 1$ s for analyzing human sleep. (**b**) REM occurs when REM-on neurons in the extended ventrolateral pre-optic area (eVLPO) inhibit REM-off neurons in ventrolateral periaquaductal gray (vlPAG) and the lateral pontine tegmentum (LPT), whose function is to actively inhibit REM-on neurons in the pre-coeruleus (PC) and parabrachial (PB) networks (dorsolateral pons). The PC and PB networks send excitatory projections to the basal forebrain (BF), hippocampus (HC) and neocortex, and to the sublateral dorsal nucleus (not shown) from which neurons project to inhibitory interneurons which produce the muscle atonia that is characteristic of REM sleep

7.2.5 Complexity Conjecture

An explicit statement of our perspective regarding the functional framework of brain electrical activity will clarify why we expected ABR to be successful.

Cognition and physiological regulation are mediated by time-dependent electrical interactions among spatially distributed neuronal networks [14–17] (Fig. 7.5). In the absence of identifiable tasks or stimuli, network connectivity is highest in wakefulness, and lower during sleep, or in subjects with neurological disease. A decrease in connectivity corresponds to an increase in deterministic activity because the brain becomes more machine-like. Complexity is decreased (deterministic activity increased) during sleep and in association with neurological disorders.

The EEG during any particular time interval is a characterization of the global electrical activity of the brain that occurred in the interval as the brain processed inputs and generated outputs. If the inputs contain contributions from specific

stimuli external to the subject, the EEG baseline brain state will contain additional transient components called evoked potentials (EPs) that are convolved with the baseline EEG. Whether characteristic changes in the determinism of the baseline EEG or transient changes in the EEG actually occurred in association with changes in the subject's metabolism or environment are empirical questions.

The law-governed activity in the EEG can be detected by time embedding in low-dimensional space whose dimensions are the instantaneously dominant brain networks (Fig. 7.5). The dimensional variables are *not* stochastic variables and therefore not generally associated with fixed probability distributions.

Next, the origins of recurrence analysis and the bases of its applicability to brain activity are described.

7.3 Recurrence Analysis

7.3.1 Historical Development

Recurrence analysis developed as a means of exploiting the recurrence plot, a graphical tool introduced to facilitate visualization of hidden patterns in time series from low-dimensional nonlinear differential equations [18]. The plot was formed by embedding a time series in dimension D using the method of time delays to produce a sequence of N D-dimensional vectors. X_i, $i = 1, 2 \ \ldots \ \mathrm{j} \ \ldots \ \mathrm{N}$. The sequence was represented in two dimensions by plotting a point at the location addressed by (i, j) whenever X_i was near X_j. The plots were said to be useful for revealing departures from autonomous behavior in physical systems such as noisy Rayleigh–Bernard-convection data or Lorenz solutions with added drift [18]. Webber and Zbilut developed a method for quantifying the plots, and repurposed them for application to biological systems [19]. The insights and innovations they described are discussed below. Application of recurrence plots to physical systems is reviewed elsewhere [20].

Webber and Zbilut recognized that outputs of biological systems exhibited aperiodic rhythmicity which was intimately related to the physiological state of the organism, but that no method existed for quantifying the rhythmicity. Linear methods were sometimes used as first approximations, but they were formally unsuitable. Linear theory assumes that variables are stochastic, and that two groups of realizations of a stochastic variable are reliably different if and only if their means differ by more than that expected on the basis of chance. But for variables governed by nonlinear differential laws, a true difference between the groups may simply be averaged away—the more measurements made or the more nonlinear the laws, the less likely a true difference will be detected. Thus linear methods are prone to obscure rather than reveal reality in those instances where it is governed by nonlinear laws, which is typically the case for biological signals.

Low-dimensional nonlinear theory similarly was no answer to the problem of quantifying aperiodic rhythmic activity (ARA) in biological time series because biological systems are invariably high-dimensional. Moreover, actual biological systems such as the brain characteristically produced non-stationary time series, a statistical property of the data which invalidated general application of the theory and rendered meaningless the results of formal processes of calculating constants of the motion.

They further observed that recurrence plots for successive time-series intervals of common physiological signals exhibited patterns which changed in a more or less regular way, suggesting that the changes in ARA were somehow dependent on the state of the organism. These realizations led them to repurpose the recurrence plot from a device that was originally designed for the exclusive purpose of detecting non-autonomous deviations in autonomous systems, to a device that could directly quantify changes in ARA in non-autonomous systems. Quantification was accomplished by means of systematic procedures that mapped geometric features of the plot into numbers.

They conjectured that the number of points in the plot relative to the possible number (the $N \times N$ array) as well as various geometric features of the plot were objective measures of the dynamical activity exhibited by biological systems. Sequential application of the quantification step then yielded recurrence time series that could be analyzed statistically, like an ordinary random variable. Thus they made biological meaning of the quantitative temporal changes exhibited by sequences of recurrence plots. In this manner, they transformed their plot measures into *bona fide* dynamical variables, an entirely novel development in the history of biological quantification. It is important to recognize that they did not claim any specific physiological meaning for the variables. On the contrary, their examples made clear that physiological meaning must be inferred empirically [19].

They defined several plot-based variables. *Percent recurrence* (%R) quantified the amount of recurrence that existed in the system during the interval that the embedded time series was generated (given the choices for the various parameters related to embedding and plot formation). Graphically, %R corresponded to the fraction of the area of the plot that contains points, but %R had no direct relation to the structure of the plot. The other variables, in contrast, were measures of the arrangement of the points.

Percent determinism (%D) characterized the number of points in the plot that fell on diagonal lines. Various possible structures in the plots have differing dynamical correlates. For example, consider three points along a diagonal (Fig. 7.6a, left panel). By definition, the *i*th and *j*th points in phase space were near, as were the consecutive states of the system (i_1, j_1 and i_2, j_2). In other words, the system's dynamics repeated for at least two successive states. The longer such behavior continues (more adjacent points along the diagonal), the stronger is our conviction that the plot reflected true law-governed activity. Vertical and horizontal lines result from the nearness of a single state to a series of other states (Fig. 7.6b, c). The diagonal line is the centrally important plot structure, probably because it has the

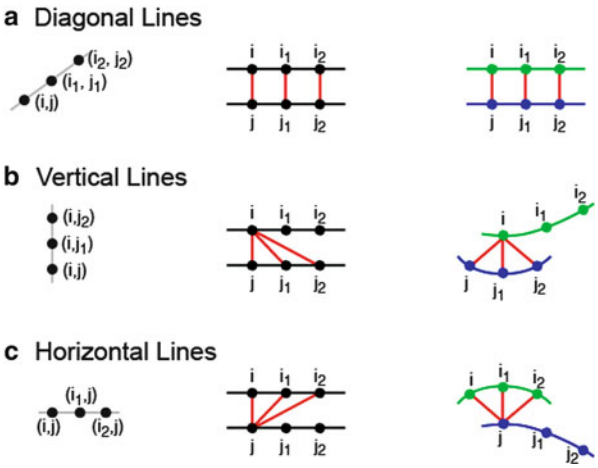

Fig. 7.6 Dynamical implications of lines in a recurrence plot. *Left column*, directions of lines in a plot. *Middle column*, schematic representation of the corresponding points in phase space. *Red lines* join points near another (based on the points shown and the definition of a plot). *Right column*, representation of the system's trajectory in phase space that produces the lines. *Blue* and *green* points are located sequentially on two different segments of the trajectory

most direct and intuitive interpretation in terms of the system's dynamical activity (Fig. 7.6a). Other variables related to the distribution of diagonal lines in a plot have also been defined [21].

Recurrence variables have no necessary relationship to dynamical theory, nor any specific meaning in relation to any standardized unit of measurement. There is no platinum bar as was accepted for the initial definition of a meter, and no acknowledged functional characterization similar to the manner in which an ohm was defined. Notwithstanding the absence of normative theories, definitions, or conventions, the variables have important and practical physiological significance that can be established directly by means of generally accepted scientific methods.

7.3.2 General Properties of Recurrence Analysis

Numerical calculations of recurrence variables from EEG signals depend on the values chosen for various parameters. There is no evidence that the principles commonly recommended for choosing parameters in connection with analysis of low-dimensional systems are optimal for analyzing the EEG. On the contrary the principles may be misleading, at least to the extent they imply that the EEG is

a stationary signal or the output of a low-dimensional system. Consequently the parameters used for ABR must be determined empirically, to maximize sensitivity for the effect sought.

The pertinent parameters include sampling frequency of the voltage time series, the window employed in the recurrence calculation, the step size used to shift the window along the time series (the shift parameter), the embedding dimension and time delay chosen for the phase-space calculations, the choice of the number of points regarded as necessary to constitute a line, and the definitions of nearness and distance (in phase space).

The sampling frequency and recurrence window used in ABR were chosen initially based on our estimates of the characteristic dynamical times in the baseline EEG and the transient response evoked in the baseline by external stimuli. Generally, %R and %D increased with increasing sampling frequency, but plateaued as a function of window size, which permitted choices of minimum window sizes that were optimal for capturing the determinism present in the signal.

Let $V_1(t)$ be an EEG interval; $\%R_1(t)$ and $\%D_1(t)$ are the corresponding percent recurrence and percent determinism time series computed from $V_1(t)$. $V_2(t)$ is a different EEG interval with corresponding recurrence times series $\%R_2(t)$ and $\%D_2(t)$. In general

$$\%R_{1,2} \neq \%R_1 + \%R_2 \tag{7.1}$$

$$\%D_{1,2} \neq \%D_1 + \%D_2 \tag{7.2}$$

where $\%R_{1,2}$ and $\%D_{1,2}$ are the recurrence time series of $V_1(t) + V_2(t)$, indicating that recurrence determinations do not follow the law of superposition. As a consequence of the non-applicability of the law of superposition, detection of the presence of a signal (an "effect" in an experiment in which a subject is exposed to a stimulus) can be manifested as any kind of a change in %R or %D relative to an appropriate control, not necessarily as a unidirectional change. In other words, in general, an effect due to a stimulus will be evidenced by a consistent change rather than by a consistent directional change.

Another important characteristic of recurrence analysis of the EEG involves the relationship between the recurrence time series and the EEG signal from which it was calculated. Assume that a signal was added to the EEG during the time window W, and that W was the window used for calculating each point in the recurrence time series (Fig. 7.7). The added signal will combine point-by-point with the baseline EEG. Some points in the recurrence time series will contain contributions from the baseline but not the added deterministic signal. In Fig. 7.7, for example, only one point in the recurrence time series includes all the determinism contributed by $V_2(t)$. Thus, in general, the time interval in the recurrence time series that contains a material contribution of the signal of interest will be shorter than the corresponding time interval in the EEG during which the signal was present.

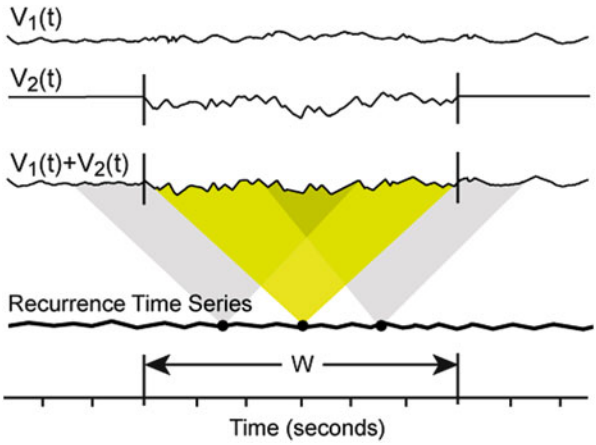

Fig. 7.7 The relationship between the EEG and its corresponding recurrence time series. $V_1(t)$ and $V_2(t)$ are continuous time series. $V_2(t)$ is non-zero during W. $V_1 + V_2$ is formed by point-wise addition of the two signals. If W is the window employed for recurrence calculations, only the center point in the recurrence time series will include all of the points in the composite that were contributed by V_2 (highlighted in *yellow*). All other points in the recurrence time series contain some points for which V_2 made no contribution, thereby lessening the overall ability of recurrence analysis to detect V_2. Typically the EEG sampling rate is 300 Hz and W is 30 points (100 ms)

7.3.3 Recurrence Analysis of Model Systems

7.3.3.1 Model Systems

The capability of recurrence analysis to detect nonlinear determinism present in the EEG can be demonstrated by adding known deterministic signals to baseline EEG, and comparing the altered time series with appropriate controls. The process models the expected determinism associated with an EP, and affords the opportunity to study the same time series before and after the addition of determinism, an impossibility in actual EP experiments.

Baseline EEGs were recorded from standard derivations in normal human subjects (Fig. 7.2), band-passed at 0.5–35 Hz (standard band for recording EEGs), and sampled at 300 Hz. The recorded signals were divided into 2-s epochs; those containing motion artifacts were discarded and artifact-free epochs were randomly selected for use in the modeling procedures. To mimic transient deterministic signals occurring in the EEG in response to sensory stimuli, sine or Lorenz signals were added to the epochs. Three types of signals were considered: (1) a 10-Hz sine added at $t = 0.85–1.15$ s to each of 50 2-s epochs such that the phase of the added signal was identical in each epoch; (2) a 10-Hz sine with a phase that varied randomly from epoch to epoch; (3) a portion of the solution from the Lorenz equation ($a = 10.14$, $r = 28$, $b = 2.67$) [22]. In each case the rms signal-to-noise (S/N) ratio was 0.4, set on an epoch-by-epoch basis.

7.3.3.2 Detection of Nonlinear Determinism

When segments of sine waves were added to EEG epochs such that the phase of the sine was always the same (negative slope starting at 0), the presence of the sine was easily detected by time-averaging (Fig. 7.8b). But when the added sine had a random phase, the added signal was not seen in the time-averaged signal (Fig. 7.8c). The same result was found when the added signal consisted of segments of a solution to the Lorenz equation (Fig. 7.8d). Thus, as expected, time-averaging was unable to reveal the presence of known deterministic signals in the cases where the signals were inconsistent (random-phase sine) or aperiodic (Lorenz). In contrast, recurrence analysis detected the addition of inconsistent or aperiodic signals, as seen by comparing the recurrence time series in the presence and absence of the added segments (Fig. 7.9).

Localization of the added determinism was affected by the choice of the recurrence window (Fig. 7.7) as well as by random fluctuations in the baseline signals. For example, the random-phase sine wave yielded simulated effects at 0.90–0.92 s and 1.05–1.15 s, even though the added deterministic signal was present through the 300-ms interval centered at 1 s (Fig. 7.10a, bottom panel). Thus only the approximate temporal location of the added determinism could be inferred from an analysis of the recurrence result. Addition of Lorenz segments also illustrated the point (Fig. 7.10b, bottom panel); in this case, statistically reliable demonstration of the added signal was even more localized in time.

Detection of deterministic changes in the EEG was improved by averaging the recurrence time series over a sliding window (called the P window, to distinguish it from the window used for recurrence calculations) prior to statistical comparisons of the *E* and *C* epochs (Fig. 7.11).

A further demonstration of the ability of ABR to detect nonlinear determinism is shown in Fig. 7.12. The presence of a Van der Pol signal (Fig. 7.12a) was averaged away in the EEGs (Fig. 7.12b) but was clearly demonstrated in %R(t) (Fig. 7.12d).

7.3.4 Overview of Recurrence Analysis of Brain Electrical Activity

Recurrence analysis quantifies order in the EEG over any desired time interval, ranging from milliseconds, as in neuroelectrophysiological studies, to intervals lasting hours that are commonly employed in clinical diagnostic procedures. We presented a broad outline of the uses and limitations of recurrence analysis, and the reasons we anticipated that the method would be experimentally and clinically useful.

The EEG necessarily differs between the presence and absence of stimuli, and between the presence or absence of neurological disorders. In the next section the

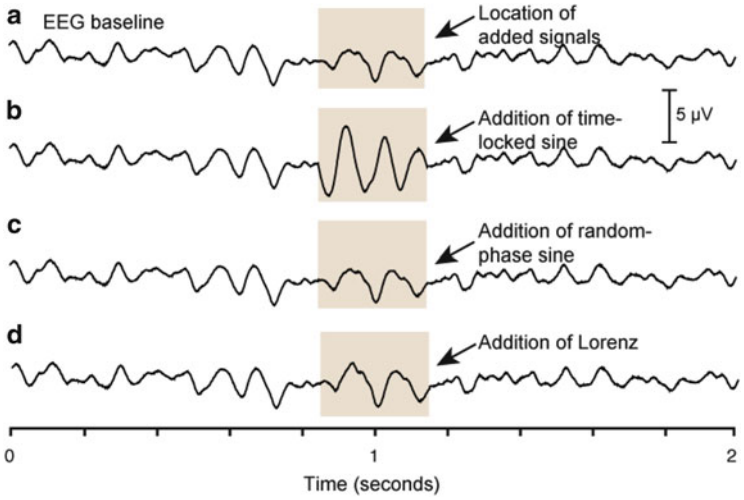

Fig. 7.8 Effect on EEG of addition of known signals. (**a**) Average of 50 2-s EEG epochs. (**b**) Effect of adding a constant-phase 10-Hz sine to each epoch, showing the effect of the averaging in revealing the presence of a phase-locked signal. (**c**) Effect of adding a random-phase sine to each epoch, showing the inability of time averaging to reveal a nonstationary signal. (**d**) Effect of adding segments of the Lorenz equation to each epoch, showing the inability of time averaging to reveal a nonlinear signal

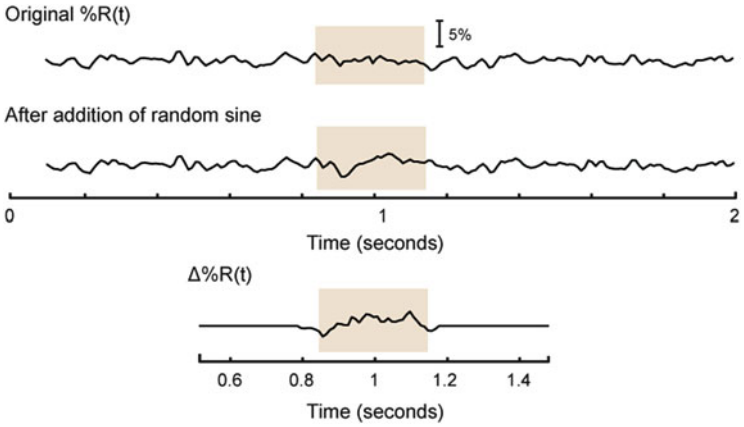

Fig. 7.9 Effect on %R(t) due to addition of nonstationary signals to the EEG. *Top*, average value of %R computed from 50 2-s EEG epochs. *Middle*, after addition of random-phase 10-Hz sine wave to each EEG epoch at t = 0.85–1.15 (*shading*). *Bottom*, time dependence of the point-wise differences of the signals before and after addition of the sine waves. Similar results were obtained following the addition of Lorenz segments. Sampling frequency 300 Hz. Embedding dimension 5. Delay five points. Recurrence window (see Fig. 7.7) 100 ms. Moving window step 1 point

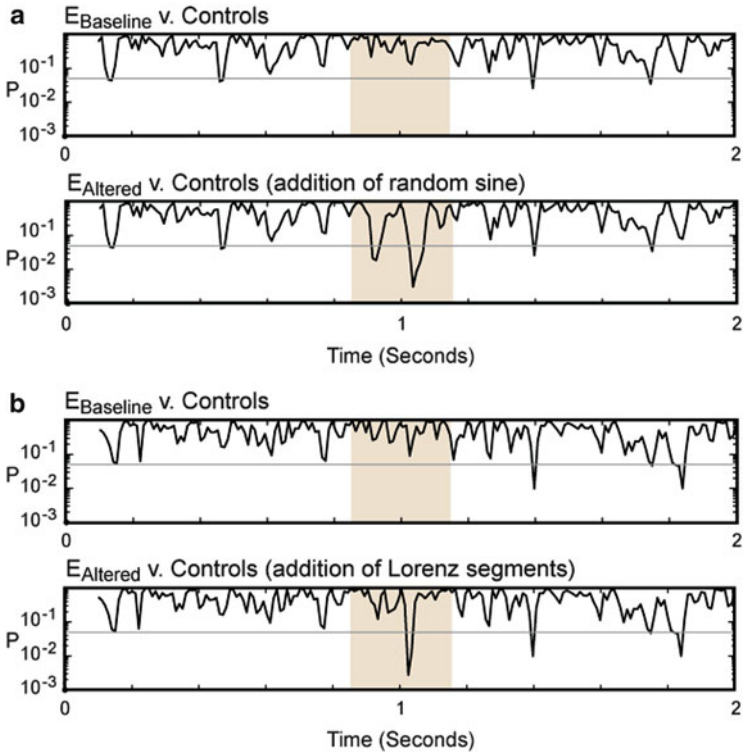

Fig. 7.10 Detection of addition of known signals to the EEG. N = 50 randomly-selected baseline epochs (*E* epochs) were compared point by point (t test) with N = 50 different randomly-selected control epochs (*C* epochs). Known determinism was added to the *E* epochs where shown (*shading*). (**a**) *E* versus *C* epochs in the absence of signals added to the *E* epochs (*top*), and after addition of random sine to the *E* epochs (*bottom*). (**b**) *E* versus *C* in the absence of signals added to the *E* epochs (*top*) and after addition of segments of the Lorenz signal to the *E* epochs (*bottom*). P, probability that the means at the indicated point in time were identical (total of approximately 600 paired t tests). Gray line, P = 0.05. The rms values of the added signals were adjusted epoch-by-epoch so that they were 40 % of the rms value of the EEG. The results show that recurrence analysis can detect the presence of a localized transient deterministic signal in the EEG with statistical certainty

goals, statistical structure, and results of experiments involving the capabilities of ABR are described. Examples are presented that evidence the ability of recurrence analysis to detect effects having profound implications for basic studies of brain activity, and that demonstrate applications of the method in translational medicine. The reader will see that recurrence analysis can produce knowledge of brain activity that is not otherwise obtainable.

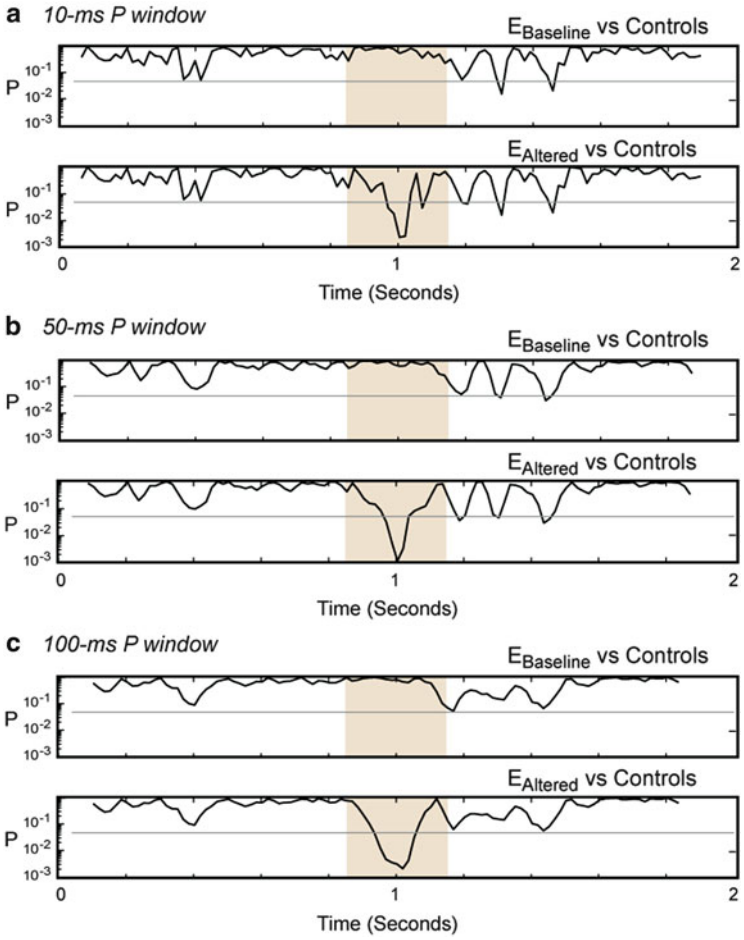

Fig. 7.11 Optimized conditions for detection of added Lorenz segments using %R. (**a**–**c**) Point-by-point statistical comparisons before and after addition of the signal to the baseline EEG, after employing the indicated P window. P, probability that the means at the indicated point in time were identical (total of approximately 600 paired t tests). Gray line, $P = 0.05$. The rms values of the added signals were adjusted epoch-by-epoch so that they were 40 % of the rms value of the EEG

7.4 Application of Recurrence Analysis

7.4.1 New Paradigm for Studying the Brain

A seminal problem in modern biology involves understanding how weak electromagnetic fields (EMFs) (fields whose strength is below the level of conscious detection) affect the growth and regulatory systems of the body, particularly the brain [23]. Early work suggested that EMFs impacted brain metabolism as

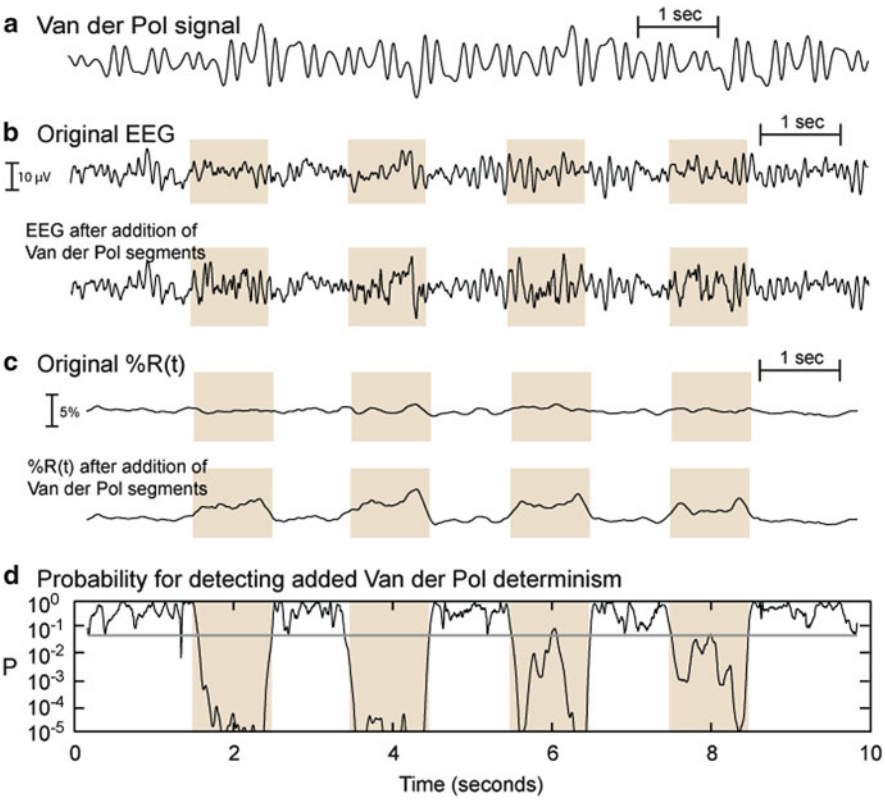

Fig. 7.12 Effects on %R(t) due to addition of Van der Pol segments to the EEG. (**a**) Representative segment of solution to Van der Pol equations. (**b**, **c**) Respectively, the EEG and %R averaged over 20 10-s EEG epochs before and after addition of 1-s Van der Pol segments where shown (*shading*) to each epoch. (**d**) Comparison of the original and altered epochs point-by-point (t-test). P, probability that the means at each indicated point in time were identical (total of 2,901 paired t tests). EEG sampling frequency 300 Hz; RQA window 50 pts; embedding dimension 5; time delay 5; radius 15 %; P value window 50 pts. Solution of the equation for the periodically driven Van der Pol oscillator $dy/dt = x - \beta x \sin(\omega t + \theta_2)$ and $dx/dt = -y - f(x) + \beta y \cos(\omega t + \theta_1)$, where $f(x) = (1/3)x^3 - \lambda x$, $\lambda = 3$, $\omega = 6.455$, $\beta = 45$, $\theta_1 = 24$, $\theta_2 = 26$. *Gray line*, $P = 0.05$

evidenced by changes in the EEG, but the traditional analytical methods of time-averaging and spectral analysis were inadequate in several respects [24].

Detection of familiar stimuli, light for example, occurs via a linear stimulus-response system. Consequently evoked potentials (EPs) triggered by common stimuli can be detected by time-averaging. But nonlinear responses cannot be efficiently detected by linear methods because they are not matched to the underlying dynamics. The first clear demonstration that EMFs consistently induced dynamical changes in brain activity was made possible by the invention of recurrence analysis, which permitted detection of nonlinear EPs [25]. Rabbits exposed to EMFs (2 G, 60 Hz magnetic field) exhibited a change in %D that was not seen directly in the

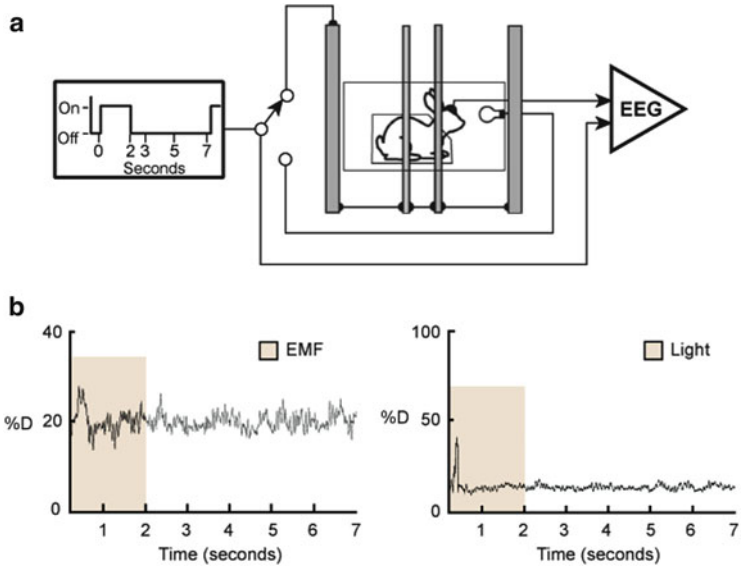

Fig. 7.13 A new paradigm for studying brain function. (**a**) Apparatus for exposing rabbits to EMF (2 G, 60 Hz magnetic field) or light (positive control stimulus). Stimuli on for 2 s during each 7-s trial. (**b**) Average %D(t) calculated from the EEG (50 trials) of a rabbit exposed to EMF (*left*) or light (*right*) [25]

EEG (Fig. 7.13). Even though the EMF was too weak to be consciously perceived, statistically significant changes were observed in all the rabbits, and the effects were manifested in both %R and %D (Fig. 7.14). Thus each of the recurrence variables captured EMF-caused law-governed activity in the EEG that could not be consistently detected by any other known method.

The generality of the phenomenon was established by showing that essentially the same results were obtained in rats [26] and human subjects [27]. In the human study, the EEG was measured from six derivations in each of eight subjects, and the effects were essentially identical regardless of the derivation. This was the expected result based on the complexity conjecture (Fig. 7.5), which assumed that each EEG was a sample measurement of the same brain state. The overall results [25–27] indicated that environmental strength EMFs could be transduced by the nervous system, resulting in subliminal changes in brain electrical activity that were consistently detectable by recurrence analysis, but not by linear methods of analysis.

7.4.2 Statistical Basis of Brain Recurrence Analysis

Application of recurrence analysis to biological time series requires an experimental and statistical framework to permit the meaning of the calculations to be ascertained.

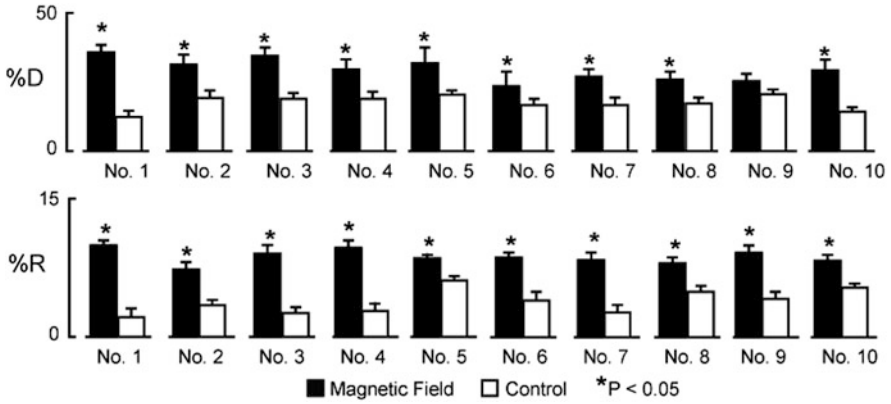

Fig. 7.14 Effect of 2 G, 60 Hz on each of 10 rabbits, 5 female (No. 1–5) and 5 male (No. 6–10) as assessed using percent determinism (%D) and percent recurrence (%R). For each rabbit and each quantifier, the difference between the exposed and control EEG epochs was evaluated using the Wilcoxon signed rank test. Window for recurrence analysis centered at 250 ms, with width of 250 ms. The average values of the quantifiers (±SD) are presented for each rabbit [25]. With one exception (%D, No. 9), statistical significance was obtained in each animal, for each recurrence variable

One approach involves comparing the experimental and control recurrence time series, point by point. For example consider a study in which EEGs were sampled at 300 Hz and analyzed to detect transient changes in brain electrical activity caused by the onset and/or offset of an auditory stimulus [28]. During independent trials, the stimulus was turned on and off and the inter-stimulus time period was used as the control for the immediately preceding stimulus period. %R(t) was extracted from the EEG and analyzed statistically to detect deterministic changes caused by the onset and offset of the stimulus.

Stimulus onset produced the expected linear EP in the time-averaged EEG, which peaked about 100 ms later (Fig. 7.15a, left panel). The EP was also seen in the probability curve, which displayed the P values point by point in the corresponding %R(t) relative to the controls (Fig. 7.15a, right panel). The EP was identified as a continuous series of tests that were pair-wise significant at $P < 0.05$. In addition, a nonlinear EP was detected (about 550 ms after stimulus onset) that was not resolved in the average EEG. Fig. 7.15b depicts an instance in which the subject did not exhibit a linear offset EP (left panel) but did exhibit a nonlinear EP detected by analysis of brain recurrence (ABR) (right panel).

Statistical considerations are critical if the ultimate goal is to make reliable, generalizable conclusions regarding the application of recurrence analysis. Simply varying embedding parameters or evaluating multiple recurrence variables yields only self-referential, non-generalizable results.

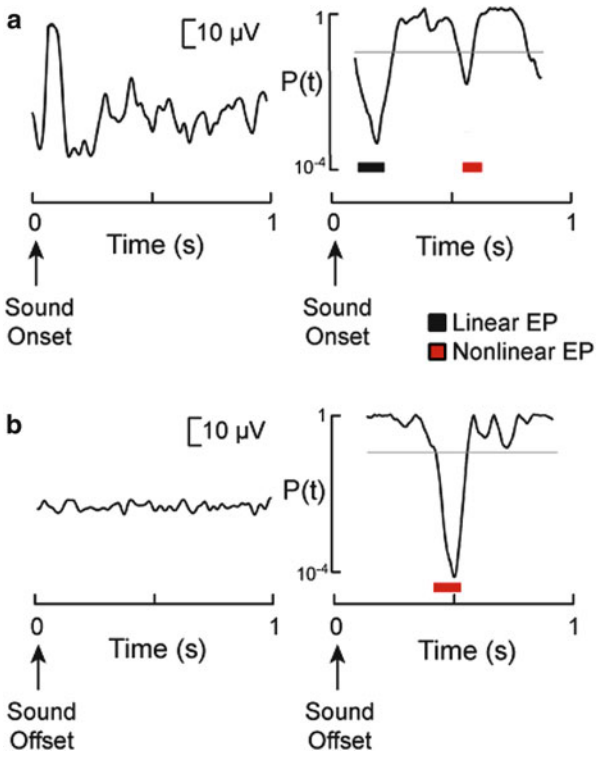

Fig. 7.15 Statistical basis for detection of auditory evoked potentials using recurrence analysis. *Left panels*, time-averaged EEG. *Right panels*, point by point probability (P) that %R(t) computed from the stimulated EEG was equal to the corresponding values computed from the controls. (**a**, **b**) EPs due to sound onset and offset, respectively [28]. *Bars* indicate EPs (>9 consecutive pair-wise significant t tests) (N = 50 trials). EP, evoked potential. *Gray line*, P = 0.05. Total of 300 t tests [28]

7.4.3 Discovery of Human Magnetic Sense

All known sensory modalities generate EPs in response to the onset and/or offset of the cognate stimulus. Consequently observations of EPs is good evidence of the existence of a sensory modality for the type of stimulus that elicited the EPs. We hypothesized the existence of a human sense capable of detecting weak magnetic fields, and used recurrence analysis to detect the EPs that we planned to interpret as evidence of the putative sensory capability.

Subjects were exposed to either sound (positive control) or a magnetic field for 2 s every 7 s (stimulus on at t = 0 and off at t = 2) (Fig. 7.16). Evoked potentials were expected within 100–400 ms of the stimuli. The control interval for both stimuli was the 1-s interval beginning at t = 5. In a study of 17 subjects, 16 subjects exhibited magnetosensory evoked potentials (MEPs) ($P < 0.05$ for *each* subject) [29]; the

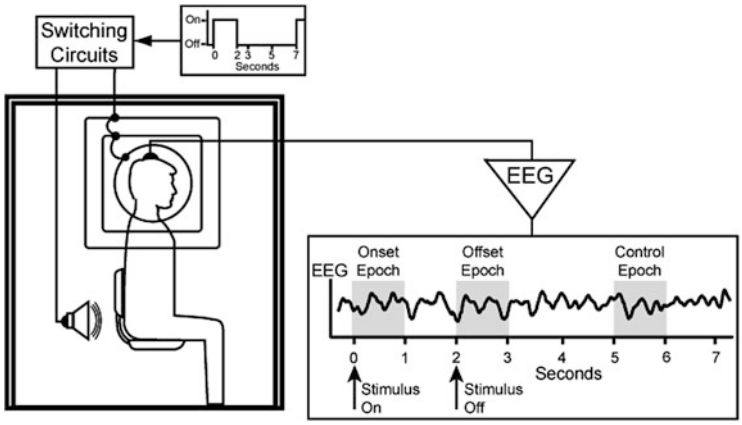

Fig. 7.16 Use of recurrence analysis to detect nonlinear magnetosensory evoked potentials. A computer-generated timing signal controlled application of the stimuli (on for 2 s, interstimulus period of 5 s). Location of onset, offset, and control epochs of a typical trial are shown. Magnetic field, generated by two sets of coils (separated by 65 cm), was homogeneous to within 5 %. Each subject had 80 trials of each stimulus [29]

latencies and durations of the EPs varied within the expected ranges, depending on the subject, and were triggered by onset and/or offset of the field. Onset results are shown in Fig. 7.17. No MEPs were detected directly in the EEG using the method of time averaging.

Because the ability to generate EPs is the hallmark of a sensory modality, the results of the study indicated that human beings can detect magnetic fields [29]. The existence of a human magnetic sense had not been discovered previously because there was no reliable method of observing nonlinear EPs prior to the development of recurrence analysis. When the new paradigm for studying the brain was employed in an appropriate statistical framework, the existence of phenomena not otherwise recognizable was validated. Both %R and %D were necessary to demonstrate the consistency of the effect. Their joint use permitted consistent detection of EPs from subject to subject, as would be expected if magnetodetection were a common human capability.

Because the study objective was fully achieved using only two recurrence variables, the other variables were not employed. In other words, %R and %D were necessary and sufficient.

7.4.4 Rationalizing Inconsistency

A question raised by the discovery of a human sensory capability for EMFs (Fig. 7.17) involved the nature of the dynamical relationship between the stimulus and the response. Field-induced changes were detected by recurrence analysis but

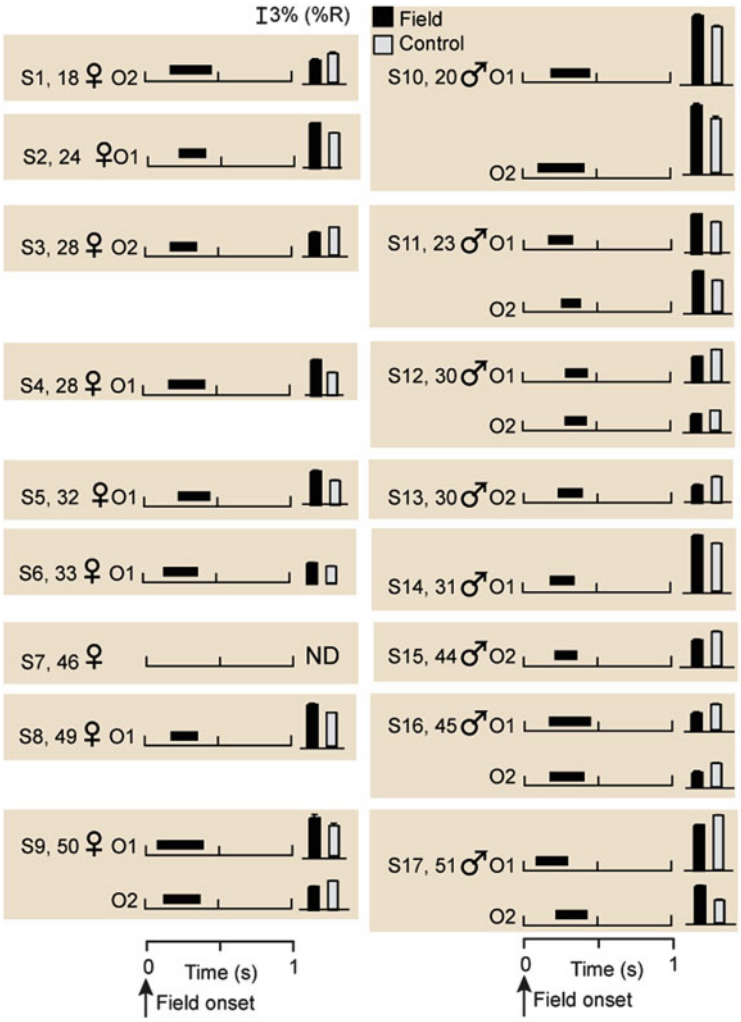

Fig. 7.17 Onset magnetosensory evoked potentials (MEPs) measured from occipital electrodes. Latency and duration in each subject are indicated by a bar over the time axis, which show the locations in the onset epochs within which individual points differed pair-wise ($P < 0.05$) from the corresponding control points. Bar graph, %R(t) (average of the significant points) (SD not resolved at scale presented). Alpha filtering was performed in nine subjects: S1, 3 (8–10 Hz), 5, 6, 9 (O1), 11, 12, 16, 17. ND, not detected [29]

not by linear methods, suggesting that responses of the subjects were governed by nonlinear laws. Nonlinear systems do not follow the law of superposition, and therefore the direction of their reactions to changes in external conditions cannot be predicted. Under the hypothesis that MEPs were nonlinearly related to the field, brain electrical responses exhibited by individual subjects would be expected to

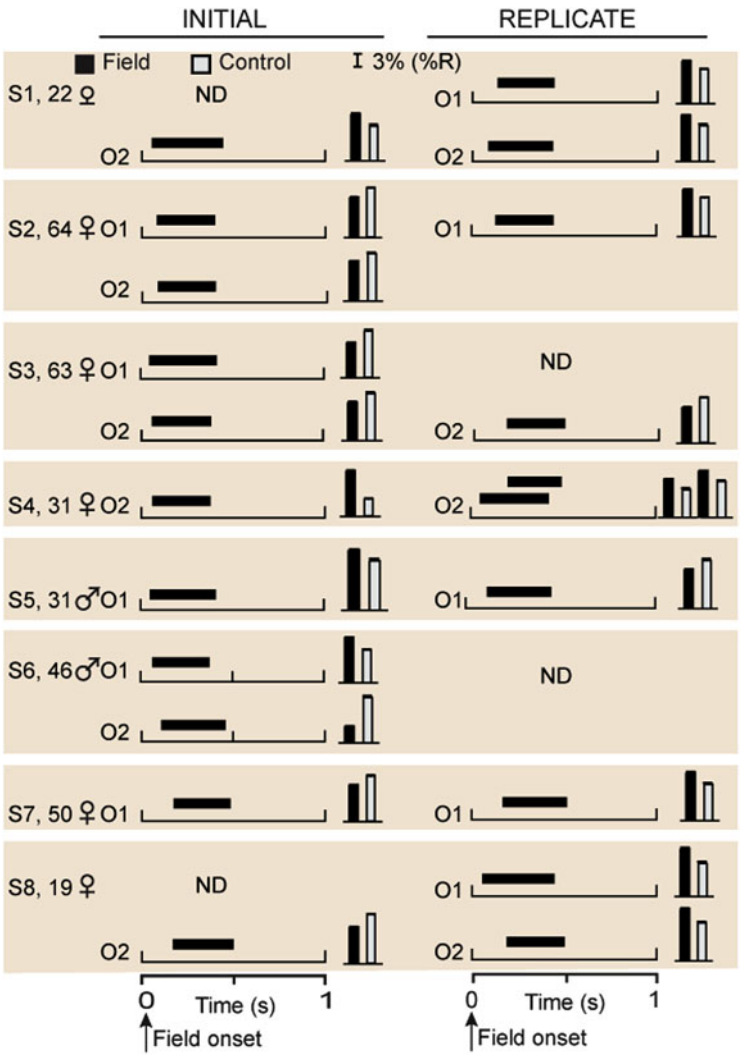

Fig. 7.18 Onset magnetosensory evoked potentials (MEP) in initial and replicate (performed at least 1 week later) studies, using recurrence analysis. Latency and duration in each subject are indicated by a bar over the time axis. Bar graphs, %R(t) (average of pair-wise significant points) (SD not resolved at scale presented). ND, not detected [30]

differ even when the experimental conditions were replicated. The hypothesis was tested in a group of eight subjects by comparing each subject's response to a specific magnetic stimulus at two times, at least 1 week apart. Intra-subject differences were observed that were of the type manifested only when the laws governing the relationship between the field and the responses were nonlinear (Fig. 7.18) [30].

Analysis of brain recurrence facilitated the discovery of new phenomena and new ways of characterizing brain activity, but ABR also had the unsettling effect of requiring a reconsideration of the process by which meaning was made from observations. Linear models of brain activity were so ubiquitous that the fundamental property of the models—adherence to the law of superposition—was often adopted as a criterion of the reliability of observations. It is not, of course, but that misconception commonly led to the false conclusion that inconsistent data (Fig. 7.17) was unreliable [31]. Reflection on the actual meaning of the reproducibility requirement of the scientific method reveals that the method requires *phenomena* be reproducible. In the present study, for example, that brain activity is reproducibly affected whenever the stimulus is applied, in accordance with the system's differential law. The reproducibility requirement applies to *data* only when the differential law is linear.

7.4.5 Canonical Conditions and ABR Variables

The optimal conditions for ABR, given the range of physiological and clinical problems considered thus far, were: sampling frequency 300–500 Hz; digital pass band 0.5–35 Hz; embedding dimension 5; delay 5; radius 15 %; scaling Euclidean; line parameter 2–20; recurrence window 30–500 points; P window 10–100 points. In all cases these canonical conditions were determined empirically, with the endpoint being the sensitivity with which the effect sought could be observed at a predetermined level of acceptability of the false-positive rate. The adopted parametric values were only bluntly optimal in the sense that reasonable departures in one or even a few choices generally had no material effect on the results. Whether future studies will require different parametric choices remains to be seen.

A further unresolved issue regarding ABR involves the potential usefulness of recurrence variables other than %R and %D. The approach we ultimately adopted regarding choices of variables was to begin with %R(t). When the putative effect sought could not be detected consistently, %D was added to the analysis, with appropriate care taken to ensure that the family-wise error rate for detecting an effect remained at the appropriate level. Use of only these variables proved sufficient to resolve all problems addressed thus far, and consequently the other suggested recurrence variables [21] have not been employed in any published studies involving ABR.

Despite the macroscale similarity of %R(t) and %D(t), use of both time series was absolutely necessary to demonstrate the consistency of the phenomena under investigation. An example is shown in Fig. 7.19 [32]. The subjects were exposed to a brief magnetic stimulus (50 ms, 60 or 30 Hz) such that the onset and offset evoked potentials (EPs) overlapped. The presence of the overlapped EPs was examined in each of six derivations from 15 subjects. For a given stimulus, say 60 Hz, six statistical tests were planned (one for each derivation) at a pair-wise significance level of 0.05. If at least three tests were significant, we planned to conclude that

the subject had exhibited an EP (family-wise error rate (PFW), 0.001). Otherwise, six additional tests were done using %D(t). Based on %R, four subjects met the a priori condition for exhibiting an EP (S1 (60 Hz), S11 (60 Hz), S12 (30 Hz), S13 (30 Hz)). When the results using %D were added, five additional cases of EP detection were revealed (S1 (30 Hz), S2 (60 Hz), S5 (30 Hz), S14 (30 Hz), S15 (60 Hz)), an inference that was justified based on consideration of the family-wise error rate. Analyses to reach the three-derivation threshold were conducted two additional times with %R and with %D, but after filtering the EEG to remove 8–10 Hz or 9–12 Hz energy (an interval that made no material contribution to the effect of the field, hence lowered the sensitivity of the t test), EPs ($\geq$3 derivations) were found in 29 of 30 cases (Fig. 7.19, *All Effects*); S14 at 60 Hz was the exception. The results were family-wise significant at $P < 0.05$ (account taken for the number of tests performed) in 26 of the 29 cases (exceptions were S6 (60 Hz), $p = 0.14$; S12 (60 Hz), $p = 0.25$; S15 (30 Hz), $p = 0.15$).

Preconditioning the EEG time series (filtering at 8–10 Hz or 9–12 Hz) combined with use of %R and %D has been sufficient to successfully resolve all experimental questions regarding analysis of brain electrical activity considered thus far.

7.4.6 Inferring Mechanisms

We proposed that human detection of EMFs was mediated by an interaction of the field with charged glycoproteins attached to the gate of an ion channel, resulting in a force that tended to open the gate (Fig. 7.20a). The proposed model had been shown to be energetically consistent with physical and thermodynamic laws and sufficiently sensitive to respond to environmental-strength EMFs [33]. The question considered was whether the mechanism was sufficiently rapid to explain the observed field-induced evoked potentials. First we measured single-channel currents in a species of fish known to be electrically sensitive and determined that the EMF-sensitive membrane ion channels opened or closed in $\sim$0.2 ms (Fig. 7.20b). We then applied a 0.2-ms magnetic stimulus to human subjects with the intent of interpreting observations of evoked potentials as evidence that the ion channel involved in field transduction was a force receptor (Fig. 7.20a).

A DC EMF that had a 10-ms rise-time and a 0.2-ms fall-time was used (Fig. 7.20c). Onset potentials were observed in all subjects, and offset potentials were observed in 60 % of the subjects [34]. These results were similar to those found earlier when both the rise- and fall-times were 10 ms [29]. We concluded therefore that the human EMF transduction system was capable of detecting fields that changed at least as rapidly as 0.2 ms (on-to-off), thus supporting the theory that transduction was directly initiated by a force receptor (Fig. 7.20a).

Time-varying magnetic fields induce electric fields in accordance with Faraday's law. Consequently *both* fields were present simultaneously in the brain in the studies involving application of magnetic fields (Figs. 7.16 and 7.20). To determine whether the electric field *alone* could explain the occurrence of the brain potentials

Subject	Stimulus (Hz)	%R	%D	%R (8-10Hz)	%D (8-10Hz)	%R (9-12Hz)	%D (9-12Hz)	All Effects	No. Tests	PFW
S1	60	O1 C4 P4	—	—	—	—	—	O1 C4 P4	6	0.001
(30F)	30	O2 C3	O2 C3	—	—	—	—	O2 O2 C3 C3	12	0.001
S2	60	O2	O2 P3	—	—	—	—	O2 O2 P3	12	0.004
(54M)	30	O1	X	C4	O1	—	—	O1 O1 C4	23	0.022
S3	60	X	C4 P3	X	O1	—	—	O1 C4 P3	22	0.047
(23M)	30	P3	P3	O2, C4	—	—	—	O2 C4 P3 P3	17	0.004
S4	60	O1	O1	C4	—	—	—	O1 O1 C4	17	0.009
(22M)	30	C3	C3	O1	—	—	—	O1 C3 C3	17	0.025
S5	60	X	X	O1	O1	C3	—	O1 O1 C3	29	0.042
(51F)	30	O1 P3	P3	—	—	—	—	O1 P3 P3	12	0.01
S6	60	C4	C4	X	X	P4	—	C4 C4 P4	27	0.14
(23M)	30	X	O1	X	X	O2 P3 P4	—	O1 O2 P3 P4	29	0.017
S7	60	X	X	O1 O2 C4 P3 P4	—	—	—	O1 O2 C4 P3 P4	18	0.001
(29F)	30	C4	C4	C3	—	—	—	C3 C4 C4	17	0.046
S8	60	X	O1	O2	O2	—	—	O1 O2 O2	23	0.003
(45F)	30	X	X	P4	P4	O2	—	O2 P4 P4	29	0.09
S9	60	C4	X	O1	O1	—	—	O1 O1 C4	22	0.028
(25M)	30	X	X	O1	O1 C4	—	—	O1 O1 C4	24	0.03
S10	60	O2	P3	C4	—	—	—	O2 C4 P3	17	0.025
(21M)	30	O2	O2	P3	—	—	—	O2 O2 P3	17	0.009
S11	60	C3 C4 P4	—	—	—	—	—	C3 C4 P4	6	0.002
(31F)	30	O2	O2	X	C4	—	—	O2 O2 C4	22	0.017
S12	60	X	X	X	P4	C4 P4	—	C4 P4 P4	26	0.251
(51F)	30	O2 P3 P4	—	—	—	—	—	O2 P3 P4	6	0.001
S13	60	X	X	O1 O2	O2 C3	—	—	O1 O2 O2 C3	24	0.003
(31F)	30	O1 O2 P3	—	—	—	—	—	O1 O2 P3	6	0
S14	60	X	X	O2 P3	X	X	X	O2 P3	24	0.286
(24F)	30	P3	C3 P3	—	—	—	—	C3 P3 P3	12	0.018
S15	60	O2	O2 C3	—	—	—	—	O2 O2 C3	12	0.004
(36M)	30	X	X	X	P3	O2	O2	O2 O2 P3	25	0.15

Fig. 7.19 Magnetosensory evoked potentials from indicated electrode derivations in 15 subjects. Column heads indicate conditions of analysis. Effects in R(t) and D(t) are shown in *red* and *green*, respectively. X, MEPs not detected. *Dashes* indicate conditions not analyzed (unnecessary because the EPs had already been detected). PFW, family-wise error. The stimulus was applied coronally to subjects S1–S10, and sagittally to subjects S11–S15 [32]

detected using ABR, we repeated the experiments, using an external electric field that produced an internal electric field but no magnetic field. The results obtained using electric fields of 27–430 V/m were identical to the results seen when magnetic fields were applied [35].

Our observation that electric fields as low as 27 V/m triggered EP that could be detected by ABR was particularly surprising because 27 V/m was roughly equivalent to the electric field induced by a magnetic field of about 10 mG, which is ubiquitous in the general environment. We confirmed this result by performing additional studies using 10 and 50 mG, and EPs were again observed (Fig. 7.21)

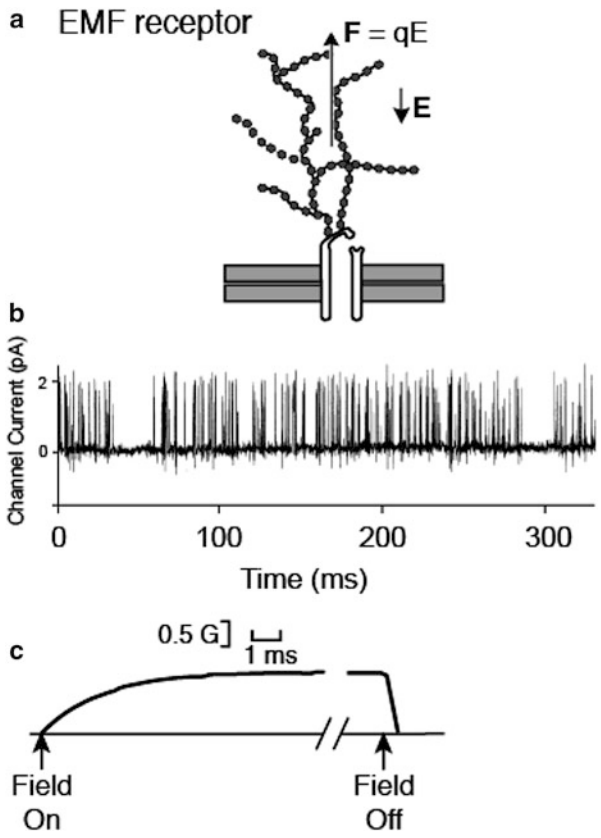

Fig. 7.20 Transduction of weak electromagnetic fields (EMFs) [33]. (**a**) Proposed EMF receptor; the rate of change of the applied magnetic field induces an electric field (E) that produces a force (F) on charged glycoproteins attached to a channel gate. (**b**) Single channel current from a voltage-sensitive channel in an electroreceptor cell in *Kryptopterus bicirrhis* (an electrosensitive species of catfish), indicating that the channel can open or close in about 0.2 ms. (**c**) Rise- and fall-times of the DC magnetic stimulus. Experimental set-up shown in Fig. 7.16

[36]. As expected, the EPs were manifested in %R(t) and %D(t) as both increases and decreases in determinism. No known method of EEG analysis other than ABR can detect this kind of dynamical change.

ABR was also capable of evidencing specific neurotransmission processes in the brain (Fig. 7.22). The hypothesis considered was that EMF detection involved synapses in the trigeminal nucleus that projected to the thalamus via glutamate-dependent pathways. If so, an anesthetic agent that antagonized glutamate neurotransmission would be expected to degrade EMF-evoked potentials (EEPs). We tested the hypothesis using ketamine which blocks glutamate receptors and xylazine which does not do so. EEGs of rats were examined using ABR to observe EEPs in the presence and absence of ketamine and xylazine anesthesia. EEPs were observed

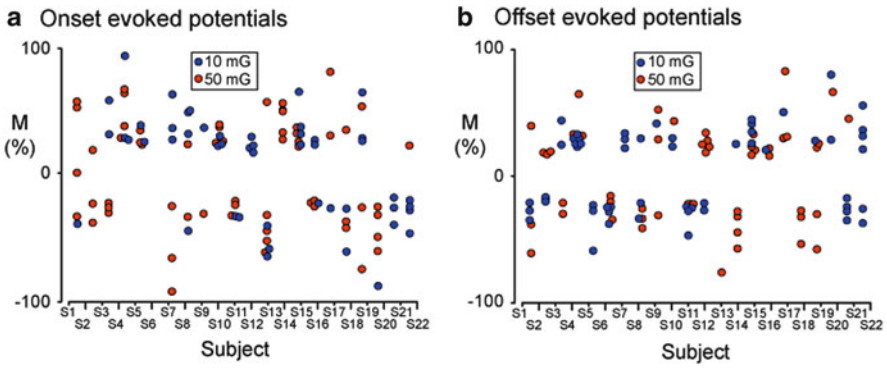

Fig. 7.21 Relative magnitude (M) of each evoked potential (expressed in percent) from each subject as determined by recurrence analysis. (**a**, **b**) Onset and offset responses, respectively. For each potential, $M = 100(E - C)/0.5(E + C)$, where E was the average of the recurrence variable (%R or %D) over the statistically significant latency interval, and C was the corresponding average in the control epoch. Where necessary, points were jittered to facilitate resolution. Values greater than 100 % are shown as 100 % [36]

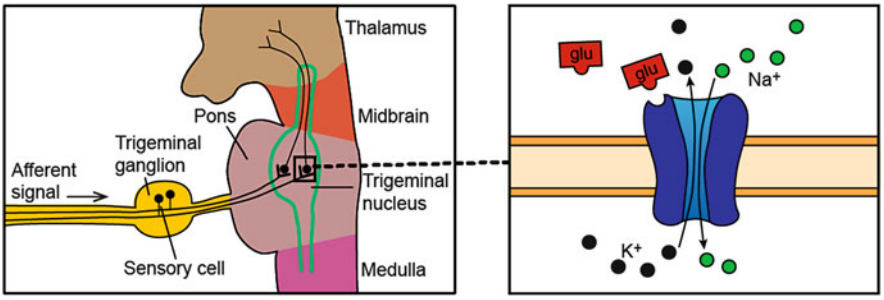

Fig. 7.22 Hypothesis regarding synaptic processes responsible for the afferent signal produced by EMF detection [37]. The afferent signal generated by EMF transduction triggers glutamate-mediated (glu) neurotransmission in the trigeminal nucleus leading to thalamic projection of the signal

in rats under xylazine anesthesia, but not when ketamine was used, indicating that the afferent signal triggered by transduction of EMFs was likely mediated by glutamate [37].

7.4.7 Cell-Phone Effects on the Brain

Questions have been raised concerning whether the electromagnetic fields emitted by cell phones could affect brain electrical activity, thereby raising the possibility that the field could ultimately lead to brain cancer or other diseases. Cell phones

emit a complicated temporal array of electromagnetic, acoustic, thermal, and tactile stimuli, any one of which might be responsible for effects on brain electrical activity that might be observed in association with cell-phone use. Thus the problem of determining whether cell-phone EMFs affect the brain requires a showing that brain activity is affected when *only* an EMF stimulus is presented, which obviates use of an actual cell phone in controlled studies.

Cell phones generate narrow pulses of high-frequency radiation that are formed by current pulses from the phone's battery. We knew that the rise- and fall-times of the pulses were within the range detectable by the nervous system [34], and that the physical process which coupled the applied magnetic field to the brain was the induced electric field generated by the rate of change of the magnetic field (Faraday's law) [35]. There was a high a priori likelihood that the brain detected the cell-phone magnetic pulses because the rate of change of the pulses produced an extraordinarily high electric field, far greater than that induced by the 60-Hz fields [36].

The question whether a *single* cell-phone pulse could be detected by the brain was addressed by applying simulated pulses in a series of independent trials, and using ABR to evaluate whether the pulses produced EPs (Fig. 7.22). Evoked potentials due to just a single cell-phone pulse were demonstrated in 18 of 20 subjects [38]. The pulse rate of a typical cell phone is 216 Hz. Consequently, the results of the study implied that 216 EPs were produced each second in the brain of a typical cell-phone user. The potential public-health implications remain to be assessed, but the salient point here is that the potential health problem could not have been detected except for ABR.

A critically important property of recurrence analysis is its applicability to *any* time series. A broad range of data manipulations may therefore be performed on the original time series or even on the computed recurrence time series, assuming that proper controls are included in the process. The possible changes include any systematic modification of the data such that features which do not contribute to recurrence-based discrimination between groups being compared are minimized, thereby increasing the sensitivity of the analysis (more likely that the effects sought will be resolved), alpha filtering for example (Fig. 7.19).

As an example of increased sensitivity based on changes in both the EEG and recurrence time series, consider a study of the effect of the high-frequency field produced by cell phones on brain electrical activity [39]. The internal antenna in a cell phone was disconnected and replaced with an external antenna positioned directly above the head of a rabbit. The antenna was energized for 2 s, with a 5-s inter-stimulus period ($N \geq 60$ 7-s trials); the last 2 s of each trial served as the control (Fig. 7.23). Both %R and %D were computed over a 300-ms window, centered at 250 ms from the beginning of the stimulus epoch. During preliminary studies involving one rabbit, the EEG and the recurrence time series were systematically altered with the goal of finding conditions of analysis that yielded statistically significant differences between the *E* and *C* epochs (Fig. 7.23). When the EEG was digitally filtered to remove 3, 4, and 8–12 Hz, and only 85 % of the attractor volume was included in the *E*–*C* comparisons, both %R and %D were significantly different

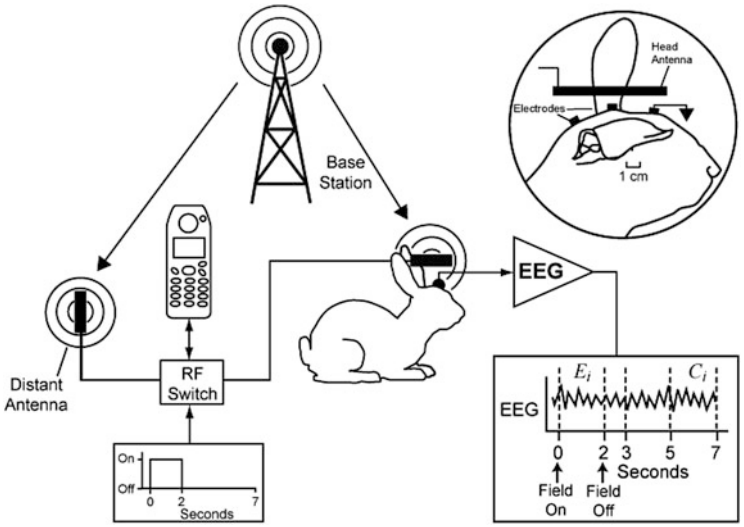

Fig. 7.23 Schematic representation of the experimental system. The detail shows the location of the electroencephalogram (EEG) electrodes relative to the head antenna [39]

($P < 0.05$). The data-conditioning procedures were then prospectively applied to nine additional rabbits and both recurrence variables were shown to be consistently altered during the exposure epochs [39].

The study demonstrated that changes in brain electrical activity associated with specific external conditions were detected more efficiently when preliminary steps were taken to precondition both the original time series and the recurrence time series to minimize signal characteristics that did not contribute to discrimination between the experimental and control data.

7.4.8 Detecting the Presence Effect

Another experimental question that can be addressed using ABR that previously could not be considered because of the absence of a suitable method for quantifying aperiodicity in the EEG is depicted in Fig. 7.24. When a stimulus is applied at $t = 0$ and removed at $t = 2$ s, nonlinear onset and offset EPs are produced that can be detected by recurrence analysis. With regard to the interval after the onset EP has decayed but while the stimulus is still present (*E* epoch), we can ask whether the *presence* of the stimulus (which entails a change in brain electrical activity) can be detected. Surprisingly, for typical stimuli such as light or sound, there is no objective method by which the subjective sense of detection (perception) can be objectively verified. By calculating %R and %D during the on-time of the stimulus but after the onset EP had decayed, objective evidence was found that confirmed the subject's subjective report of stimulus perception (hence confirming the change

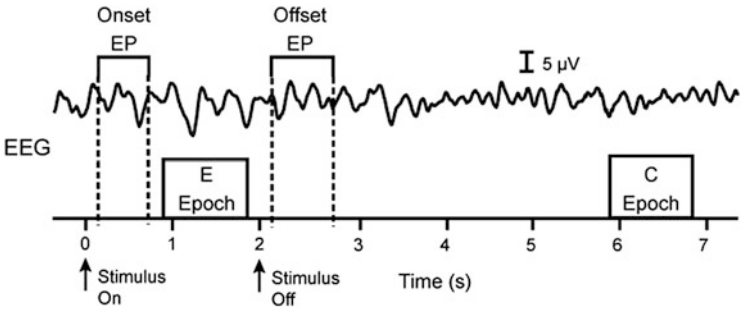

Fig. 7.24 Detection of changes in the EEG induced by the *presence* of a stimulus. EEG trial showing the locations of the epochs used to study the physiological effect of the presence of a stimulus (in distinction to the transient effect caused by its onset and offset). *EP*, evoked potential; *E*, exposed; *C*, control [40]

a) *Sound Stimulus*				
Subject	Age/Gender	%D	%R	V_{rms}
S1	30/M	O1 C3 C4 P3	O1 C3 C4 P3	ND
S2	45/M	O1 O2 C3 C4 P3 P4	O2 C3 C4 P3 P4	ND
S3	32/F	O1 O2 C4 P4	ND	ND
S4	29/F	ND	C3 C4 P4	ND
S5	28/F	O1 C3 C4 P3	O1 P4	O1 C3 C4 P3
b) *Field Stimulus*				
Subject	Age/Gender	%D	%R	V_{rms}
S6	18/F	O1 C3 C4 P3 P4	ND	ND
S7	30/M	O1 O2 C3 C4 P3 P4	O1 P3 P4	ND
S8	50/F	O1 O2 C3 C4 P3 P4	ND	ND
S9	49/F	O1 O2 C3 C4 P3 P4	O1 O2 P3 P4	ND
S10	46/F	O1 C3 C4 P3	ND	ND
c) *Light Stimulus*				
Subject	Age/Gender	%D	%R	V_{rms}
S11	51/F	C3 P4	ND	ND
S12	29/M	ND	ND	ND
S13	50/M	ND	O1 C4	C4 P4
S14	46/F	O1 O2 P3 P4	ND	ND
S15	31/F	O1 C4	ND	ND

Fig. 7.25 Detection of the presence effect. Light onset and offset were at $t = 0$ and $t = 2$ s, respectively. Using nonlinear (%D, %R) and linear (V_{rms}) analysis, brain electrical activity at 0.7–1.7 s was compared with that at the inter-stimulus epoch (3.7–4.7 s) for each of the six derivations from each subject. Effects in %R(t), %D(t) are shown in *red* and *green*, respectively. The derivations for which the comparisons differed significantly ($p < 0.05$) are listed. The presence effect was not detected by linear analysis (V_{rms}) except in S5 and S13 [40]

in brain electrical activity). The same conditions of analysis permitted an objective verification of a change in brain electrical activity when an EMF was applied (a subliminal stimulus for which the subjects cannot report the subjective sensation of perception) (Fig. 7.25). Thus ABR offers the possibility to study the dynamics of continuous detection (perceptual and non-perceptual) of external stimuli (the *presence effect*).

7.4.9 Diagnosing Multiple Sclerosis

Multiple sclerosis (MS) is an immune-system-mediated disease that degrades brain structure, leading to serious clinical consequences. We hypothesized that the neuronal networks involved in attention to stimuli onset and/or offset would be affected by the presence of MS, and that the effect could be detected by ABR. An onset response to an EMF stimulus occurred in only 27 % of a group of MS patients studied, compared with 90 % in the control group (Fig. 7.26). Further, ABR analysis of the baseline EEG in both groups provided additional evidence that the two groups could be distinguished; mean %R was 30 % greater in the MS group, and %D was 15 % greater [42]. In principle, EEG analysis could provide the basis of a functional method for detecting organ-level changes in brain activity associated with MS even before the changes were detected by imaging brain structure.

7.4.10 Applications in Sleep Medicine

Human sleep is commonly studied by analyzing simultaneously digitized signals from the brain, heart, skeletal muscle, and other physiological systems [43]. Sleep macroarchitecture is characterized by examining the signals in 30-s epochs and classifying them on the basis of standardized rules into one of four mutually exclusive stages, either rapid-eye-movement (REM) sleep or progressively deeper stages of non-REM sleep respectively termed N1, N2, and N3; the other recognized stage is wake after sleep onset (WASO) [44]. A graphical record of the distribution of sleep-stage changes during overnight sleep, termed a hypnogram (Fig. 7.27, bottom panel) provides sleep-medicine specialists an overview of the macroarchitecture of the night's sleep. Knowledge of sleep-stage distributions permits normal and pathological sleep to be distinguished [46].

The concept of sleep stage is fundamental to an understanding of sleep physiology, but has several limitations. Staging emphasizes a discontinuity of sleep, leading to its representation as a discrete process rather than a continuous process which is actually the case. Second, sleep staging is rule-determined [44], and application of the rules depends on observer judgment; typical average inter-rater agreement among experts is 80–85 %. Finally, and probably most importantly, the non-REM stages are defined in terms of the behavior of the EEG, whereas REM sleep is defined in terms of the coordinated behavior of three signals, only one of which is the EEG. This fundamental difference prevented characterization of sleep stages in terms of a single, continuous, objective, physiological variable. ABR provides a complementary perspective on sleep characterization that is based solely on EEG metrics [47].

For application of ABR to the sleep EEG, %R and %D were calculated second-by-second and then averaged over 30-s epochs, resulting in approximately 900 values for a typical 8-h sleep study. The results, when viewed graphically, reveal

a) Participants with multiple sclerosis		
Participant	Onset Stimulus	PFW
1 (40)	NE	—
2 (34)	NE	—
3 (52)	NE	—
4 (32)	O1 O2 C3 C3 C4	0.003
5 (19)	NE	—
6 (30)	O2 O2 C3	0.029
7 (18)	NE	—
8 (27)	C3 C4 P4	0.029
9 (50)	NE	—
10 (31)	NE	—
11 (38)	NE	—
b) Participants who had no medical complaints		
Participant	Onset Stimulus	PFW
1 (51)	O2 O2 C3	0.031
2 (66)	O2 C3 C3 P4	0.001
3 (22)	NE	—
4 (26)	C3 C4 C4 P3	0.001
5 (23)	C3 C4 P4	0.001
6 (23)	C3 C3 C4 C4	0.001
7 (23)	O1 C3 C3 P3	0.004
8 (46)	O1 O1 C3	0.005
9 (23)	O1 O2 C4 C4 P3 P4	0.000
10 (25)	P3 P3 P4	0.084

Fig. 7.26 Changes in brain electrical activity induced by EMF stimuli. NE, No effect. PFW, family-wise error. Age (years) in parentheses. Effects in %R(t), %D(t) are shown in *red* and *green*, respectively. Stimulus was a subliminal electric field [41]

the expected ultradian macroarchitecture (2–5 relative maxima), and associated fine structure not determinable in the standard hypnogram (Fig. 7.27, top panel). When the individual epoch values were color coded based on the clinically-assessed sleep stage, both %R and %D had their highest values during deep sleep (N3), lowest values during wake, with the other stages exhibiting intermediate values (Fig. 7.27). Thus %R and %D provided a continuous measure of sleep depth, which is a crucially important variable in determining sleep quality. The generality of the phenomenon was established by evaluating values of %R and %D as a function of sleep stage in 20 patients (Fig. 7.28).

The results (Fig. 7.28) suggested a possible basis for the use of ABR for diagnosing sleep disorders. Obstructive sleep apnea (OSA) is a disorder characterized

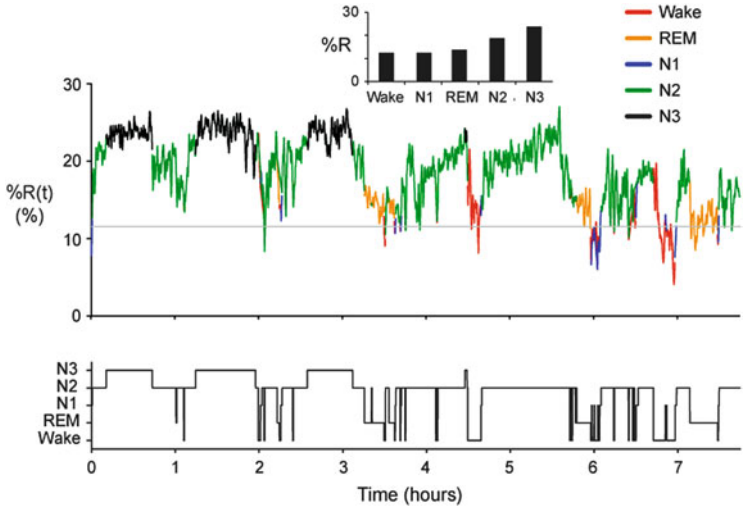

Fig. 7.27 Typical percent recurrence %R(t) in the EEG (C3) from an overnight sleep study of a patient with OSA (AHI = 9.4). Percent recurrence was calculated every second, averaged epoch-by-epoch, and color-coded by sleep stage (hypnogram, *lower panel*). For clarity in presentation, the curve was smoothed using a Savitzky–Golay filter. Gray line (%R = 11.6) indicates average value of percent recurrence from clinically normal subjects during wake [45]. Insert shows sleep-stage-specific average values of percent recurrence. OSA, obstructive sleep apnea. AHI, apnea–hypopnea index (accepted clinical measure of OSA severity)

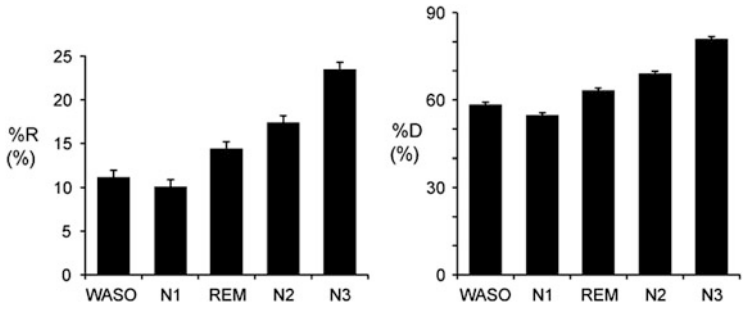

Fig. 7.28 Sleep-stage-specific percent recurrence (%R) and percent determinism (%D) in the EEGs (C3) from 20 patients with OSA (AHI 5–30). The recurrence values were computed second-by-second from each patient and averaged across sleep stage. Grand averages (±SE) [45]

by periodic collapse of the upper airway during sleep, resulting in intermediate hypoxemia, hypercarbia, and variable degrees of sleep disruption. Blood oxygen levels are affected almost immediately by apneic events, resulting in afferent signals to the brain that initiate appropriate compensatory responses. These autonomic

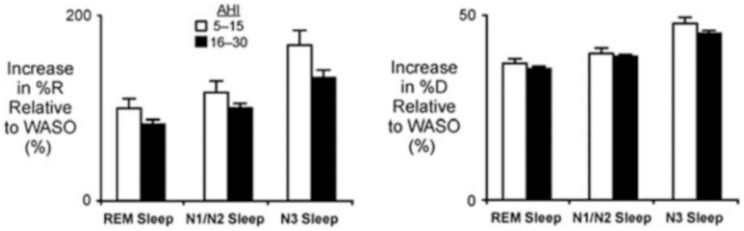

Fig. 7.29 Effect of OSA severity on sleep-stage-specific changes in %R and %D. Both recurrence variables were computed second-by-second from the EEG (C3), normalized by the patient's value during WASO, and averaged over ten patients with mild OSA (AHI 5–15) and ten patients with moderate OSA (AHI 16–30). The N1 and N2 stages were combined. Sleep-stage-specific means ± SE [45]

processes are necessarily accompanied by changes in the functional state of the brain, compared with what the state would otherwise have been.

We expected that the changes could be detected in patients with more severe OSA, and Fig. 7.29 demonstrates that this was indeed the case; the increases in %R and %D during sleep (associated with deeper and hence more restful sleep) were less in all sleep stages in patients with more severe OSA.

Individual sleep-stage-specific ABR markers for sleep depth (Fig. 7.28) cannot presently sustain a diagnosis of a sleep disorder because of inter-patient variations. But when the diagnostic/prognostic power associated with individual sleep-stage-based recurrence markers is combined in the context of a suitable statistical design, successful prediction becomes possible. For example, ABR was used to construct four time series from an overnight EEG, namely %R(t), %D(t), and two additional time series based on measures of their time-dependent variances. Combining the four time series with the five sleep stages yielded a total of 20 markers. When the markers were analyzed using linear discriminant analysis, the resulting biomarker function was 100 % accurate in diagnosing patients with either mild or moderate OSA [45].

7.5 Summary

The aperiodic rhythmic activity (ARA) displayed in the EEG has long been suspected to code for specific physiological processes. A plethora of methods for discerning the latent meaning of the EEG have been proposed, but ultimately they were unsuccessful in yielding a general approach to the problem of interpreting the EEG. A novel solution became possible following the development of recurrence analysis. The techniques developed to study the dynamics of low-dimensional systems were applied in a model-free fashion to the study of time series outputs from high-dimensional systems, the premier example of which is the EEG generated by the brain. Using recurrence analysis, we developed ABR, an approach that

quantitates ARA without explicit resort to specific dynamical models, in distinction to traditional approaches such as Fourier decomposition which assumes that the ARA are composed of parts (individual frequencies), and in distinction to chaos theory which assumes that the ARA arises from low-dimensional dynamical activity. In the context of controlled statistically-based experiments that addressed specific hypotheses, ABR was consistently useful in helping to understand brain function. Examples of such studies were described in the preceding section.

The usefulness of ABR ultimately stems from its incorporation of an additional analytical step in the process of analyzing the EEG. The nature of this additional step merits reflection. Two fundamental aspects of the scientific method for determining true cause–effect relationships (and studies of brain metabolism are no exception) involve the concepts of *averaging* and *replication*. Identification of a cause–effect relationship requires multiple independent observations of a phenomenon under controlled circumstances, and the combining of the observations by means of averaging. The point in the analysis where the averaging should be performed is a critically important but underappreciated issue. In experiments involving linear systems, the dependent variable is stochastic and consequently its values can be averaged directly to form a mean that may properly be regarded as the true characteristic behavior of the system. The *replication* requirement is satisfied by showing that the mean value can be reproduced (more or less) at will. But when the system under consideration is nonlinear, the dependent variable is *not* a stochastic variable. In this case repeated measurements under the same conditions do not yield necessarily similar values because the law of superposition does not generally apply to nonlinear systems. As a consequence of this common behavior of nonlinear systems, successively determined means *in principle* are not replicates. Consequently direct resort to averaging for purposes of evaluating the relation between the independent and dependent variables can have the opposite effect of that intended—obscuring knowledge of the system's determinism rather than revealing it (Fig. 7.8). ABR obviates this problem by interposing a second dependent variable (derived algorithmically from the directly-measured variable) that captures and quantifies the experimentally-induced determinism (the difference between the E and C groups in a controlled study) *prior* to averaging. Consequently each independent trial can contribute to the requisite sensitivity needed to rationalize the existence of an effect, because each trial adds to the ability to distinguish the determinism of interest from background signals (signals that do not depend on the presence of the independent variables) (Fig. 7.12). In many cases of experimentally-induced nonlinear determinism, the scientific requirement of replication is fulfilled by a showing that the *phenomenon* (as opposed to the magnitude and/or sign of a mean) is replicable. Examples of this behavior have been discussed (Figs. 7.18 and 7.21).

The studies discussed in the previous section demonstrated ABR can be exploited to yield a broad range of useful results in the areas of basic and translational neuroscience.

References

1. S.M. Blinkov, I.I. Glezer, *Human Brain in Figures and Tables*, 1st edn. (Basic Books, New York, 1968)
2. R.W. Williams, K. Herrup, The control of neuron number. Annu. Rev. Neurosci. **11**, 423–453 (1988)
3. E. Bullmore, O. Sporns, Complex brain networks: graph theoretical analysis of structural and functional systems. Nat. Rev. Neurosci. **10**(3), 186–198 (2009)
4. O.V. Kolomytkin, A.A. Marino, Neurobiophysics, in *Handbook of Molecular Biophysics: Methods and Applications*, ed. by H.G. Bohr (Wiley-VCH, Hoboken, 2009), pp. 523–556
5. E.L. Reilly, EEG recording and operation of the apparatus, in *Electroencephalography: Basic Principles, Clinical Applications, and Related Fields*, ed. by E. Niedermeyer, F. Lopes da Silva (Lippincott Williams & Wilkins, Philadelphia, 2004)
6. S. Luck, E.S. Kappenman, *The Oxford Handbook of Event-Related Potential Components* (Oxford University Press, New York, 2013)
7. T. Yamada, E. Meng, *Practical Guide for Clinical Neurophysiologic Testing* (Lippincott Williams & Wilkins, New York, 2011)
8. H. Pratt, A. Starr, H.J. Michalewski, N. Bleich, N. Mittelman, The auditory P50 component to onset and offset of sound. Clin. Neurophysiol. **119**(2), 376–387 (2008)
9. F. Bandini, M. Pierantozzi, I. Bodis-Wollner, Parkinson's disease changes the balance of onset and offset visual responses: an evoked potential study. Clin. Neurophysiol. **112**, 976–983 (2001)
10. B.A. Clementz, A. Keil, J. Kissler, Aberrant brain dynamics in schizophrenia: delayed buildup and prolonged decay of the visual steady-state response. Cogn. Brain Res. **18**, 121–129 (2004)
11. E. Tanaka, K. Inui, T. Kida, R. Kakigi, Common cortical responses evoked by appearance, disappearance and change of the human face. BMC Neurosci. **10**, 38–46 (2009)
12. J. Gleick, *Chaos* (Penguin, New York, 2008)
13. W.S. Pritchard, D.W. Duke, Measuring chaos in the brain: a tutorial review of nonlinear dynamical EEG analysis. Int. J. Neurosci. **67**, 31–80 (1992)
14. C. Büchel, K.J. Friston, Dynamic changes in effective connectivity characterized by variable parameter regression and Kalman filtering. Hum. Brain Mapp. **6**(5–6), 403–408 (1998)
15. A.M. Kelly, L.Q. Uddin, B.B. Biswal, F.X. Castellanos, M.P. Milham, Competition between functional brain networks mediates behavioral variability. Neuroimage **39**(1), 527–537 (2008)
16. C.M. Lewis, A. Baldassarre, G. Committeri, G.L. Romani, M. Corbetta, Learning sculpts the spontaneous activity of the resting human brain. Proc. Natl. Acad. Sci. U. S. A. **106**(41), 17558–17563 (2009)
17. Y. Liu, J.H. Gao, M. Liotti, Y. Pu, P.T. Fox, Temporal dissociation of parallel processing in the human subcortical outputs. Nature **400**(6742), 364–367 (1999)
18. J.-P. Eckmann, S.O. Kamphorst, D. Ruelle, Recurrence plots of dynamical systems. Europhys. Lett. **4**, 973–979 (1987)
19. C.L. Webber Jr., J.P. Zbilut, Dynamical assessment of physiological systems and states using recurrence plot strategies. J. Appl. Physiol. **76**, 965–973 (1994)
20. M.C. Casdagli, Recurrence plots revisited. Physica D **108**(1–2), 12–44 (1997)
21. J.P. Zbilut, C.L. Webber Jr., Recurrence quantification analysis, in *Wiley Encyclopedia of Biomedical Engineering*, ed. by M. Akay (Wiley, Hoboken, 2006), pp. 2979–2986
22. H.D. Abarbanel, Nonlinear systems, in *Encyclopedia of Applied Physics*, ed. by G.L. Trigg (VCH Publishers, New York, 1994), pp. 417–439
23. R.O. Becker, A.A. Marino, *Electromagnetism & Life* (State University of New York Press, Albany, 1982)
24. G.B. Bell, A.A. Marino, A.L. Chesson, Alterations in brain electrical activity caused by magnetic fields: detecting the detection process. Electroencephalogr. Clin. Neurophysiol. **83**, 389–397 (1992)
25. A.A. Marino, E. Nilsen, C. Frilot, Consistent magnetic-field induced changes in brain activity detected by recurrence quantification analysis. Brain Res. **951**, 301–310 (2002)

26. C. Frilot II, S. Carrubba, A.A. Marino, Magnetosensory function in rats: localization using positron emission tomography. Synapse **63**, 421–428 (2009)
27. A.A. Marino, E. Nilsen, A.L. Chesson Jr., C. Frilot, Effect of low-frequency magnetic fields on brain electrical activity in human subjects. Clin. Neurophysiol. **115**, 1195–1201 (2004)
28. S. Carrubba, C. Frilot, A. Chesson, A. Marino, Detection of nonlinear event-related potentials. J. Neurosci. Methods **157**, 39–47 (2006)
29. S. Carrubba, C. Frilot, A.L. Chesson Jr., A.A. Marino, Evidence of a nonlinear human magnetic sense. Neuroscience **144**, 356–367 (2007)
30. S. Carrubba, C. Frilot, A.L. Chesson Jr., A.A. Marino, Nonlinear EEG activation by low-strength low-frequency magnetic fields. Neurosci. Lett. **417**, 212–216 (2007)
31. A.A. Marino, C. Frilot, Comment on "Proposed test for detection of nonlinear responses in biological preparations exposed to RF energy". Bioelectromagnetics **24**, 70–72 (2003)
32. S. Carrubba, C. Frilot, A.L. Chesson Jr., C.L. Webber Jr., J.P. Zbilut, A.A. Marino, Magnetosensory evoked potentials: consistent nonlinear phenomena. Neurosci. Res. **60**, 95–105 (2008)
33. O.V. Kolomytkin, S. Dunn, F.X. Hart, C. Frilot, D. Kolomytkin, A.A. Marino, Glycoproteins bound to ion channels mediate detection of electric fields: a proposed mechanism and supporting evidence. Bioelectromagnetics **28**, 379–385 (2007)
34. A.A. Marino, S. Carrubba, C. Frilot, A.L. Chesson Jr., Evidence that transduction of electromagnetic field is mediated by a force receptor. Neurosci. Lett. **452**, 119–123 (2009)
35. S. Carrubba, C. Frilot II, F.X. Hart, A.L. Chesson Jr., A.A. Marino, The electric field is a sufficient physical determinant of the human magnetic sense. Int. J. Radiat. Biol. **85**, 622–632 (2009)
36. S. Carrubba, C. Frilot II, A.L. Chesson Jr., A.A. Marino, Numerical analysis of recurrence plots to detect effect of environmental-strength magnetic fields on human brain electrical activity. Med. Eng. Phys. **32**(8), 898–907 (2010)
37. C. Frilot II, S. Carrubba, A.A. Marino, Sensory transduction of weak electromagnetic fields: role of glutamate neurotransmission by NMDA receptors. Neuroscience **258**, 184–191 (2014). http://dx.doi.org/10.1016/j.neuroscience.2013.11.009
38. S. Carrubba, C. Frilot II, A.L. Chesson Jr., A.A. Marino, Mobile-phone pulse triggers evoked potentials. Neurosci. Lett. **469**, 164–168 (2010)
39. A.A. Marino, E. Nilsen, C. Frilot, Nonlinear changes in brain electrical activity due to cell-phone radiation. Bioelectromagnetics **24**, 339–346 (2003)
40. S. Carrubba, C. Frilot II, A.L. Chesson Jr., A.A. Marino, Method for detection of changes in the EEG induced by the presence of sensory stimuli. J. Neurosci. Methods **173**, 41–46 (2008)
41. S. Carrubba, A. Minagar, E. Gonzalez-Toledo, A.L. Chesson Jr., C. Frilot II, A.A. Marino, Multiple sclerosis impairs ability to detect abrupt appearance of a subliminal stimulus. Neurol. Res. **32**, 297–302 (2010)
42. S. Carrubba, A. Minagar, A.L. Chesson Jr., C. Frilot II, A.A. Marino, Increased determinism in brain electrical activity occurs in association with multiple sclerosis. Neurol. Res. **34**(3), 286–290 (2012)
43. M.H. Kryger, T. Roth, W.C. Dement, *Principles and Practice of Sleep Medicine* (Saunders, Philadelphia, 2010)
44. American Academy of Sleep Medicine (2007) *The AASM Manual for the Scoring of Sleep and Associated Events: Rules, Terminology and Technical Specifications*. American Academy of Sleep Medicine
45. P.Y. Kim, D.E. McCarty, L. Wang, C. Frilot II, A.L. Chesson Jr., A.A. Marino, Two-group classification of patients with obstructive sleep apnea based on analysis of brain recurrence. Clin. Neurophysiol. **125**, 1174–1181 (2014). doi:10.1016/j.clinph.2013.11.002
46. S. Chokroverty, R.J. Thomas, M. Bhatt, *Atlas of Sleep Medicine*, 1st edn. (Elsevier, Philadelphia, 2005)
47. L. Wang, P.Y. Kim, D.E. McCarty, C. Frilot II, A.L. Chesson Jr., S. Carrubba, A.A. Marino, EEG recurrence markers and sleep quality. J. Neurol. Sci. **331**, 26–30 (2013)